

Identifying Sparse Treatment Effects

Yujin Jeong

Emily Fox

Ramesh Johari

Abstract

Based on technological advances in sensing modalities, randomized trials with primary outcomes represented as high-dimensional vectors have become increasingly prevalent. For example, these outcomes could be week-long time-series data from wearable devices or high-dimensional neuroimaging data, such as from functional magnetic resonance imaging. This paper focuses on randomized treatment studies with such high-dimensional outcomes characterized by sparse treatment effects, where interventions may influence a small number of dimensions, e.g., small temporal windows or specific brain regions. Conventional practices, such as using fixed, low-dimensional summaries of the outcomes, result in significantly reduced power for detecting treatment effects. To address this limitation, we propose a procedure that involves subset selection followed by inference. Specifically, given a potentially large set of outcome summaries, we identify the subset that captures treatment effects, which requires only one call to the Lasso, and subsequently conduct inference on the selected subset. Via theoretical analysis as well as simulations, we demonstrate that our method asymptotically selects the correct subset and increases statistical power.

1 Introduction

Due to technological advances in sensing modalities, randomized controlled trials with primary outcomes represented as high-dimensional vectors have become increasingly prevalent; examples include time series data from wearable sensors (e.g., heart rate or glucose levels), or neuroimaging sensor data. When trial outcomes are high-dimensional, the scientist faces a challenge: in which dimension(s) is there a treatment effect, if any? On one hand, the scientist could pre-commit to a small number of dimensions and test for treatment effects there (e.g., a fixed window of time in the wearables setting). However, this risks missing the treatment effect. On the other hand, if the entire set of dimensions is considered, then finding treatment effects amounts to searching for a needle in a haystack.

In this paper, we consider the problem of causal inference from experimental data with high-dimensional outcomes. Our emphasis is on the development of a practical technique that allows the scientist to consider the entire high-dimensional outcome, and yet successfully identify and estimate sparse treatment effects. We present a practical, easily deployed method that identifies the subset of outcome representations that contain the treatment effect given a large pool of outcome representations, and then carries out inference for the treatment effect on the selected subset.

In the remainder of this section, we present some motivation for our approach with examples from real-world experiments and semi-synthetic experiment. First, we observe that for interpretability, instead of working with the raw outcomes, scientists often study a compressed representation of the raw data. A common practice is to compress the outcomes into a one-dimensional representation of interest, $Y \in \mathbb{R}$; alternatively, one can consider p one-dimensional representations, concatenated as $Y \in \mathbb{R}^p$, where p is small, and employ multiple testing. This practice is illustrated in the examples below.

1. **Time series data from wearable devices.** Over the last decade, continuous glucose monitoring (CGM) has become an essential component of diabetes management for many people with type 1 diabetes. The study by [Aleppo et al. \(2017\)](#) investigates whether the use of CGM without confirmatory blood glucose monitoring (BGM) measurements is as safe and effective as using CGM adjunctive to BGM in adults with well-controlled type 1 diabetes through a randomized controlled experiment. Their primary outcome was time-in-range, abbreviated as TIR, (the percentage of time when the patient’s blood glucose level lies between 70–180 mg/dL) over the

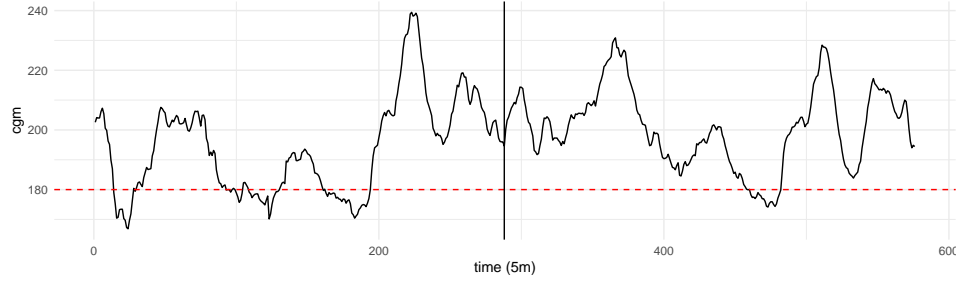


Figure 1: An example trace representing the daily average of CGM data in week 1 (before solid vertical line) and week 2 (after the solid vertical line). The time series is recorded every 5 minutes, resulting in $24 \times 12 = 288$ points before and after the potential intervention time (solid vertical line).

26-week period of monitoring. In this study, the raw outcome Y^{raw} is a time series of glucose measurement over 26 weeks, and their choice of one-dimensional representation of outcomes Y_1 is time-in-range (70–180 mg/dL) over the 26-week period.

2. **Neuroimaging data.** Neuroscientists often investigate the impact of external stimuli on brain activity using neuroimaging techniques, such as functional magnetic resonance imaging (fMRI). In such cases, outcomes are high-dimensional in the form of images or time series of images.

For example, [Koenig et al. \(2017\)](#) studies the effects of the insulin sensitizer metformin on Alzheimer’s disease through a randomized placebo-controlled crossover design. Arterial Spin Label MRI data, which measures cerebral blood flow (CBF) in different brain regions, was collected at week 0 as baseline and at week 8. Then the researchers tested whether the treatment had significant effects on CBF in 21 pre-defined regions of interest. In this study, the raw outcome Y^{raw} is a pre-processed brain image and their choice of representation of outcomes, $Y \in \mathbb{R}^{21}$, is measured CBF in 21 regions of interest.

In another example, [Anand et al. \(2005\)](#) studies the effects of the antidepressant sertraline on corticolimbic connectivity using a matched pairs experimental design. They obtained a series of fMRI scans (512 time points) at week 0 as baseline and week 6. Then the researchers compared correlation coefficients between the time series of four different regions of interest and tested whether there are significant differences between the control and treatment groups. In this study, the raw outcome Y^{raw} is a time series of brain images and their choice of representation, $Y \in \mathbb{R}^{\binom{4}{2}=6}$, is a vector of correlation coefficients between four different regions of interest.

This practice of considering one or a few outcome representations is common when scientists are interested in a few specific representations based on their scientific motivation. However, if scientists are interested in unraveling how the treatment effect may manifest in the high-dimensional outcome space and picking the right representation, this practice may fail to capture the treatment effect when the treatment effect is sparse.

To demonstrate this issue caused by not knowing which outcome representation is appropriate, we generate a semi-synthetic scenario to simulate realistic treatment effects observable in a clinical system for managing type 1 diabetes. We use CGM data from the ongoing 4T study at Stanford’s Lucille Packard Children’s Hospital. In this study, patients are reviewed by clinicians weekly and, if an adjustment is deemed necessary, the clinician will send a message. These messages represent the interventions and often their effects may be time-localized, such as a correction to overnight hyperglycemia. To mimic this scenario, we generate synthetic treatment effects as follows. We randomly select 10,000 two-week long CGM traces, each providing recordings every 5 minutes, and retain the 5,000 traces with minimal missing data. We treat the first week’s data as a pre-treatment time series and the second week’s as post-treatment. Each week’s data is then averaged across days in the week in a time-aligned fashion to create a 24-hour average CGM representation that can be used to highlight the potential impacts of interventions on specific times of the day. An example CGM trace is shown in Figure 1. We created treatment and control groups by randomizing treatment assignment with a 50% probability of receiving a treatment. To create the synthetic treatment effect, we localize an effect around lunchtime by reducing glucose levels of the treated units by 5 units between 12pm and 2pm,

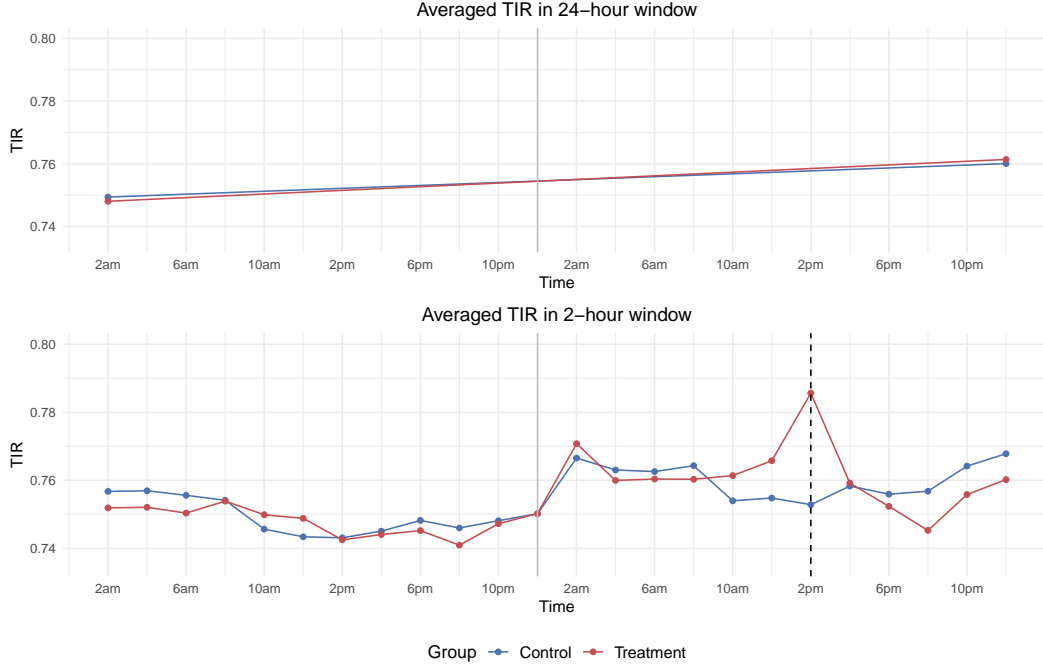


Figure 2: The averaged TIR for both the control group and the treatment group where there is a synthetic treatment effect applied between 12pm and 2pm. The dashed line indicates a lunchtime. The plot above shows that TIRs computed with 24-hour time windows fail to capture the treatment effect. On the other hand, the plot below implies that TIRs computed with two-hour time windows may capture the treatment effect.

simulating a lunchtime intervention. Note that the intervention of reducing glucose levels will increase TIR for patients with hyperglycemia.

If a scientist considers a one-dimensional summary, TIR (the percentage of time when the patient’s blood glucose level lies between 70–180 mg/dL) over 24 hours, the treatment signal is lost as the treatment effect is sparse. This is illustrated in Figure 2. On the other hand, TIR calculated with a two-hour time window seems to be able to capture the sparse treatment effect. In practice, however, the scientist might not know the duration and location of the actual treatment effect.

1.1 Our Objective and Approach

We consider a setting where the treatment effect is sparse, meaning that the treatment effect manifests in only a few directions in the high-dimensional outcome space \mathbb{R}^d . Moreover, we suppose that the scientist does not know which outcome representation can effectively capture the treatment effect. In the example in the previous section, this is when a scientist is uncertain about both the duration and the location of the treatment effect.

Without knowing relevant representations, we suppose that scientists consider a vector of p different representations, where p is large. If p is small, it is more likely that a vector of representations does not include representations that can capture the sparse treatment effect. However, if p is large, then even though there is a higher chance of inclusion of representations that capture the treatment effect, the multiple testing correction factor can be substantial.

Our main contribution in this paper is a practical method for identification of the representations where a treatment effect manifests when the number of representations p is large. In our setting, we assume that scientists have p one-dimensional outcome summaries (i.e., representations) $Y \in \mathbb{R}^p$ where p can be even larger than n . This large pool of outcome summaries may be defined using background knowledge. There are also several representation learning methods for high-dimensional data including time-series and image data sets (Bengio et al., 2013).

Because p is large, we consider a *sample splitting* method. In the first split, the data scientist finds

a large pool of outcome summaries and selects a subset in which the treatment effect may manifest. In the second split, they estimate the treatment effect on the selected subset. Our method primarily focuses on the subset selection process: how to choose a subset of outcome representations in which the treatment effect may manifest. We introduce a sparse regression approach for subset selection, where we employ a regularized weighted linear regression with carefully chosen weights. We show that our method can recover the subset of outcome representations consistently. From simulated experiments, we demonstrate the effectiveness of our method, particularly when the treatment effect is relatively weak.

Before continuing to the technical presentation, below we revisit the examples from real-world experiments to illustrate how this subset selection process can be applied.

1. **Time series data from wearable devices (continued).** In diabetes treatment, certain interventions may be effective within specific time ranges, such as mornings, post-meal periods, or during sleep. Alternatively, treatments might be effective under specific hypoglycemia or hyperglycemia conditions. In such scenarios, the treatment effect may be reflected in time-in-range (TIR) metrics defined within particular glucose ranges and time frames. If a data scientist is uncertain about the precise glucose levels and time periods affected by the treatment, they may consider various TIR metrics targeting different glucose ranges and time frames, resulting in a vector of outcome representations, $Y \in \mathbb{R}^p$, where p is large. If the treatment effect is sparse, using subset selection methods, one may identify a subset of outcome representations where the treatment effect potentially manifests.
2. **Neuroimaging data (continued).** If scientists aim to gain a more comprehensive understanding of the impact of drug treatment on the brain, they might explore a larger number p of brain regions of interest. For large p , the dimension of outcome representations becomes p and $p(p-1)/2$ in [Koenig et al. \(2017\)](#) and [Anand et al. \(2005\)](#), respectively. If we set aside the sample size issues mentioned in the original papers and assume we have sufficient sample sizes, it is possible, once again, to identify a subset of outcome representations where the treatment effect potentially manifests utilizing subset selection methods.

1.2 Outline of the Paper

In Section 2, we discuss related work. In Section 3, we introduce the formal setting of the paper. In Section 4, we provide an overview of a baseline approach for how a data scientist might select a subset of outcomes where the treatment effect potentially manifests. Section 5 outlines our proposed method based on sparse regressions. Section 5.1 provides the insight behind the proposed procedure, while Section 5.2 presents theoretical results. We conclude in Section 6 where we evaluate the performance of our proposed procedure on synthetic and semi-synthetic data sets.

2 Related Work

This work falls into the general randomized controlled setting in causal inference ([Imbens and Rubin, 2015](#)). In randomized controlled experiments, linear regression has been employed to improve the precision of average treatment effect estimators through linear regression adjustments with pre-treatment covariates ([Deng et al., 2013](#); [Lin, 2013](#); [Jin and Ba, 2023](#)). [Bloniarz et al. \(2016\)](#) and [Wager et al. \(2018\)](#) have a discussion of high-dimensional regression adjustments when there are a large number of pre-treatment covariates. Our paper also studies high-dimensional regression techniques within randomized controlled experiments, but we focus on the setting where outcomes are high-dimensional instead of pre-treatment covariates.

One of the most popular high-dimensional linear regression technique is the Lasso introduced by [Tibshirani \(1996\)](#). Conditions for oracle inequalities for the Lasso have been studied by [Bunea et al. \(2007\)](#), [van de Geer \(2008\)](#), [Zhang and Huang \(2008\)](#), [Meinshausen and Yu \(2009\)](#), and [Bickel et al. \(2009\)](#). Furthermore, variable selection properties of the Lasso have been investigated by [Meinshausen and Bühlmann \(2006\)](#), [Zhao and Yu \(2006\)](#), [Lounici \(2008\)](#), and [Wainwright \(2009\)](#). In addition,

sample-splitting and subsequent statistical inference procedures have been developed in Wasserman and Roeder (2009) and Meinshausen et al. (2008).

The average treatment effect estimator investigates the mean difference between the treated group and the control group. Therefore, our work is also closely related to high-dimensional mean testing (the problem of testing whether a population mean μ equals to some known vector μ_0 under the high-dimensional regime) (Huang et al., 2022). Among the array of high-dimensional mean testing methods, our work is closely related to the projection test (Lopes et al., 2011; Huang, 2015; Liu et al., 2022). This approach involves mapping the high-dimensional samples to a lower-dimensional space and subsequently applying traditional methods, such as Hotelling’s T^2 to the projected samples. Our paper adopts a causal inference perspective, exploring the interplay between treatment assignments, pre-treatment covariates, and post-treatment outcomes. Moreover, we employ a linear regression specification, which is more practical for practitioners to implement using tools such as `glmnet` in R.

3 Preliminaries

We consider a setting with n individuals. Each individual receives a single binary treatment of interest $T_i \in \{0, 1\}$, and we observe a subsequent outcome vector, denoted by $Y_i \in \mathbb{R}^p$, for each individual. (Note that in our motivating examples, this p -dimensional outcome is a vector of different representations derived from a raw observed outcome vector $Y_i^{\text{raw}} \in \mathbb{R}^d$; in our development, we treat Y_i as our primary outcome.) In our setting, the outcome representation is high-dimensional: we allow the dimension p to increase with n . In our subsequent presentation, we will also consider the inclusion of pre-treatment covariates $X_i \in \mathbb{R}^m$ for each individual.

Following the potential outcomes framework (Imbens and Rubin, 2015), each individual has a p -dimensional pair of potential outcomes: $(Y_i(0), Y_i(1))$. We take a super-population perspective where

$$(X_i, Y_i(0), Y_i(1)) \stackrel{\text{i.i.d}}{\sim} \mathbb{P}.$$

Moreover, we consider randomized controlled trials where $P(T_i = 1) = \pi$ (independently across i , with $0 < \pi < 1$) and

$$T_i \perp \{Y_i(0), Y_i(1)\}.$$

We assume that π is bounded away from zero and one. Moreover, assume that the realized outcomes are

$$Y_i = T_i Y_i(1) + (1 - T_i) Y_i(0).$$

The (super-population) average treatment effect (ATE) is defined as

$$\tau := \mathbb{E}[Y(1) - Y(0)] \in \mathbb{R}^p.$$

Estimation and Inference of ATE. Here, we review the standard approach to estimating and inferring τ when the dimension of the outcome, p , does not increase at the same rate as n and $p \ll n$. The standard approach to estimation of τ is to consider the *difference-in-means* estimator:

$$\hat{\tau}_{\text{DiM}} = \frac{1}{n_t} \sum_{i=1}^n T_i Y_i(1) - \frac{1}{n_c} \sum_{i=1}^n (1 - T_i) Y_i(0), \quad (1)$$

where $n_t = \sum_i T_i$ is the number of treated samples and $n_c = \sum_i (1 - T_i)$ is the number of control samples.

Inference for $\hat{\tau}_{\text{DiM}}$ is obtained using a standard application of the central limit theorem. Formally, we have:

$$\sqrt{n}(\hat{\tau}_{\text{DiM}} - \tau) \rightarrow N(0, \Sigma_{\text{DiM}})$$

where

$$\Sigma_{\text{DiM}} = \frac{1}{\pi} \text{Var}(Y(1)) + \frac{1}{1 - \pi} \text{Var}(Y(0)),$$

which can be consistently estimated as:

$$\begin{aligned}\hat{\Sigma}_{\text{DiM}} &= \frac{n}{n_t} \cdot \frac{1}{n_t} \sum_{i:T_i=1} \left(Y_i(1) - \frac{1}{n_t} \sum_{i:T_i=1} Y_i(1) \right) \left(Y_i(1) - \frac{1}{n_t} \sum_{i:T_i=1} Y_i(1) \right)^\top \\ &+ \frac{n}{n_c} \cdot \frac{1}{n_c} \sum_{i:T_i=0} \left(Y_i(0) - \frac{1}{n_c} \sum_{i:T_i=0} Y_i(0) \right) \left(Y_i(0) - \frac{1}{n_c} \sum_{i:T_i=0} Y_i(0) \right)^\top.\end{aligned}\quad (2)$$

Inference can be made for each component j of the outcome, Y_j , with the usual z-test and multiple testing. The p-value for testing the null hypothesis $H_{0j} : \tau_j = 0$ that there is no treatment effect on Y_j , is defined as

$$P\left(Z \geq \sqrt{n}(\hat{\Sigma}_{\text{DiM},jj})^{-1/2}|\hat{\tau}_{\text{DiM}j}|\right) \cdot p,$$

where Z is the standard Gaussian random variable and p is a multiple testing correction factor.

Inference can also be made for a group of outcomes. This involves the following statistic, referred to as the Hotelling T^2 statistic, which generalizes the usual t -test:

$$n\hat{\tau}_{\text{DiM}}^\top (\hat{\Sigma}_{\text{DiM}})^{-1} \hat{\tau}_{\text{DiM}}. \quad (3)$$

Under the null hypothesis $H_0 : \tau = 0$ that there is no treatment effect, the Hotelling T^2 statistic in (3) follows the chi squared distribution with p degrees of freedom. Thus, the p-value for testing the null hypothesis H_0 is defined as

$$P\left(\chi^2(p) \geq n\hat{\tau}_{\text{DiM}}^\top (\hat{\Sigma}_{\text{DiM}})^{-1} \hat{\tau}_{\text{DiM}}\right) \quad (4)$$

where $\chi^2(p)$ is the chi-squared random variable with p degrees of freedom.

Our objective. We conclude this section by noting that, as discussed in the introduction, we are primarily interested in settings where the treatment effect may be *sparse* within the p -dimensional outcome. Formally, throughout the remainder of the paper, we suppose that there exists a set of dimensions S_τ such that the sparsity index of S_τ is $|S_\tau| := s_\tau < p$ and

$$\begin{aligned}\mathbb{E}[Y_j|T=1, X] &= \mathbb{E}[Y_j|T=0, X] \quad \text{for } j \notin S_\tau, \\ \mathbb{E}[Y_j|T=1, X] &\neq \mathbb{E}[Y_j|T=0, X] \quad \text{for } j \in S_\tau.\end{aligned}$$

Our goal in this paper is to present a practical regression-based method for approximate recovery of S_τ , together with valid inference on treatment effects localized to the identified subset. In Section 1, we provided motivation for the use of a sample-splitting approach, where half the data sample is used to identify S_τ , and the second half of the data sample is used for inference. Next, we present a simple, commonly employed baseline approach for this purpose (first without, then with pre-treatment covariates); we subsequently compare our proposed approach to this baseline.

4 A Baseline Approach

In this section we present a simple, commonly used baseline approach that serves as a reference point. For simplicity, we assume that the data scientist knows (or has a bound) on the sparsity s_τ .

The most common method employed for subset identification is to rank outcomes by their treatment effect sizes, and select outcomes with the largest effect sizes. This is equivalent to considering the following objective:

$$\hat{\beta} = \underset{\beta}{\operatorname{argmin}} \left\| \left(\frac{\hat{\tau}_{\text{DiM}j}}{\sqrt{\hat{\Sigma}_{\text{DiM}jj}}} \right)_{j=1}^p - \beta \right\|_2^2 \quad \text{subject to } \|\beta\|_0 \leq s_\tau, \quad (5)$$

where $\|\beta\|_0 = \sum_{j=1}^p 1\{\beta_j \neq 0\}$ is the ℓ_0 norm of β . Then, the estimated \hat{S}_τ is defined as

$$\hat{S}_\tau = \{j | \hat{\beta}_j \neq 0\},$$

which is simply the top s_τ outcomes based on the effect sizes of average treatment effects.

Having identified a subset \hat{S}_τ on the first data split, inference can proceed as in Section 3 on the second data split, but restricted to the set \hat{S}_τ . We can specialize the definitions in (1) and (2) to the subset \hat{S}_τ , and carry out inference using the second data split as suggested in (3) or (4) defined with these \hat{S}_τ -specific quantities. Note that in (3), we would still apply a correction factor for multiple testing, but it is significantly smaller, especially when $|\hat{S}_\tau|$ is much smaller than p .

Going beyond the basic method above, in causal inference, the pre-treatment covariates are often leveraged to reduce the variance of the treatment effect estimators (Deng et al. (2013), Lin (2013), Jin and Ba (2023)). As an example, the CUPED estimator (Deng et al., 2013) estimates τ as

$$\hat{\tau}_{\text{CUPED}j} = \frac{1}{n_t} \sum_{i=1}^n T_i(Y_{ij}(1) - \hat{\theta}_j^\top(X_i - \bar{X})) - \frac{1}{n_c} \sum_{i=1}^n (1 - T_i)(Y_{ij}(0) - \hat{\theta}_j^\top(X_i - \bar{X})),$$

where $\hat{\theta}_j$ is the vector of OLS coefficients of a linear regression of Y_{ij} , the pooled outcomes of control and treatment groups, on pre-treatment covariates X_i , for $j = 1, \dots, p$. Note that \bar{X} is the mean of covariates on the pooled data.

Lin's estimator (Lin, 2013) improves the CUPED estimator by running separate regressions in the treated and control groups, with the agnostic property that it does not induce higher variance than the difference-in-mean estimator without any model assumptions. Lin's estimator estimates τ as

$$\hat{\tau}_{\text{Lin}j} = \frac{1}{n_t} \sum_{i=1}^n T_i(Y_{ij}(1) - \hat{\theta}_j^{1\top}(X_i - \bar{X})) - \frac{1}{n_c} \sum_{i=1}^n (1 - T_i)(Y_{ij}(0) - \hat{\theta}_j^{0\top}(X_i - \bar{X})),$$

where $\hat{\theta}_j^w$ ($w = 0$ or 1) is the vector of OLS coefficients of a linear regression of $Y_{ij}(w)$ on the pre-treatment covariates X_i , for $j = 1, \dots, p$.

Note that both the CUPED estimator and Lin's estimator can be written similarly to the difference-in-means estimators as

$$\hat{\tau}_{\text{method}j} = \frac{1}{n_t} \sum_{i=1}^n T_i \tilde{Y}_{ij}(1) - \frac{1}{n_c} \sum_{i=1}^n (1 - T_i) \tilde{Y}_{ij}(0),$$

where for the CUPED estimator, \tilde{Y}_{ij} is defined as

$$\tilde{Y}_{ij} = Y_{ij} - \hat{\theta}_j^\top X_i \quad (6)$$

and for Lin's estimator, \tilde{Y}_{ij} is defined as

$$\tilde{Y}_{ij} = Y_{ij} - \frac{n_c}{n} \hat{\theta}_j^{1\top} X_i - \frac{n_t}{n} \hat{\theta}_j^{0\top} X_i. \quad (7)$$

To adapt the baseline approach to use pre-treatment covariates, instead of the simple difference-in-mean estimator, one can use covariates-adjusted difference-in-mean estimators. For either CUPED or Lin's method ($\text{method} \in \{\text{CUPED}, \text{Lin}\}$), we consider the following objective:

$$\hat{\beta} = \underset{\beta}{\operatorname{argmin}} \left\| \left(\frac{\hat{\tau}_{\text{method}j}}{\sqrt{\hat{\Sigma}_{\text{method}jj}}} \right)_{j=1}^p - \beta \right\|_2^2 \quad \text{subject to } \|\beta\|_0 \leq s_\tau.$$

The variance estimate is defined as (2) but with \tilde{Y} instead of Y . Then, again $\hat{S}_\tau = \{j | \hat{\beta}_j \neq 0\}$.

With these definitions, inference proceeds again as in Section 3 using the second split with covariates-adjusted \tilde{Y} , but restricted to the set \hat{S}_τ .

Under some regularity and model assumptions (as in Section 5.2), this baseline approach would consistently recover S_τ as $n \rightarrow \infty$ (similarly as in Section 5.2). In our numerical simulations in Section 6.1, however, we see that the baseline approach may not work well in low signal-to-noise-ratio (SNR) regimes (see Figure 3). Notably, many sensor data examples outlined in Section 1 fall within such low SNR regimes. In the next section, we propose subset selection methods using the Lasso, which is known to generally perform well in low SNR regimes (Hastie et al., 2020).

5 Our Proposed Approach: Subset Selection via Sparse Regression

Our approach starts from the following observation: Rather than considering each individual outcome representation separately, they can be considered as a group as represented by the Hotelling's T^2 test statistic in (3). This leads us to consider the following objective:

$$\hat{S}_\tau = \max_S \hat{\tau}_{\text{DiM}}^S \text{ }^\top (\hat{\Sigma}_{\text{DiM}}^S)^{-1} \hat{\tau}_{\text{DiM}}^S \quad \text{subject to } |S| \leq s_\tau, \quad (8)$$

where $\hat{\tau}_{\text{DiM}}^S$, $\hat{\Sigma}_{\text{DiM}}^S$ on the right-hand side are computed for each set S .

In the next subsection, we show that in fact the preceding problem is equivalent to fitting a weighted linear regression with carefully chosen weights W_i as

$$\hat{\beta} = \underset{\beta}{\operatorname{argmin}} \frac{1}{n} \sum_i W_i (T_i - (Y_i - \bar{Y})^\top \beta)^2 \quad \text{subject to } \|\beta\|_0 \leq s_\tau, \quad (9)$$

where $\|\beta\|_0 = \sum_{i=1}^p 1\{\beta_i \neq 0\}$ is the ℓ_0 norm of β and $\hat{S}_\tau = \{j | \hat{\beta}_j \neq 0\}$. Note that we have treatment assignments as response variables and centered outcomes as explanatory variables. Here, \bar{Y} is the mean of outcomes on the pooled data.

Now that we have reformulated the problem as a weighted linear regression with subset selection, we can employ various statistical tools such as forward subset selection, backward subset selection, and Lasso. In the following, we focus on Lasso.

Unlike the objective (5) which has a closed-form solution, solving (9) often presents computational complexity challenges. To avoid this issue, we develop our method using Lasso. The Lasso solves a convex relaxation of (9) where we replace the ℓ_0 norm with the ℓ_1 norm as

$$\hat{\beta} = \underset{\beta}{\operatorname{argmin}} \frac{1}{n} \sum_i W_i (T_i - (Y_i - \bar{Y})^\top \beta)^2 \quad \text{subject to } \|\beta\|_1 \leq t$$

where $\|\beta\|_1 = \sum_{i=1}^p |\beta_i|$, and $t \geq 0$ is a tuning parameter. Due to convex duality, the above problem is equivalent to the more common penalized form

$$\hat{\beta} = \underset{\beta}{\operatorname{argmin}} \frac{1}{n} \sum_i W_i (T_i - (Y_i - \bar{Y})^\top \beta)^2 + 2\lambda \|\beta\|_1 \quad (10)$$

where $\lambda \geq 0$ is a tuning parameter. Again, $\hat{S}_\tau = \{j | \hat{\beta}_j \neq 0\}$.

Having identified a subset \hat{S}_τ on the first data split, inference can proceed as in Section 3 using the second data split, but restricted to the set \hat{S}_τ . We can specialize the definitions in (1) and (2) to the subset \hat{S}_τ , and carry out inference using the second data split as suggested in (3) or (4) defined with these \hat{S}_τ -specific quantities. Note that in (3), we would still apply a correction factor for multiple testing, but this will be significantly smaller after our subset selection step when $|\hat{S}_\tau| \ll p$.

The pre-treatment covariate adjusted version of our proposed method is straightforward: we directly include pre-treatment covariates in the regression. In particular, for the Lasso, instead of (10), we fit a weighted Lasso of treatment assignments on centered outcomes and centered covariates as follows:

$$(\hat{\beta}, \hat{\alpha}) = \underset{\beta, \alpha}{\operatorname{argmin}} \frac{1}{n} \sum_i W_i (T_i - (Y_i - \bar{Y})^\top \beta - (X_i - \bar{X})^\top \alpha)^2 + 2\lambda \|\beta\|_1 \quad (11)$$

where the ℓ_1 penalty is on β and $\lambda \geq 0$ is a tuning parameter. Then, $\hat{S}_\tau = \{j | \hat{\beta}_j \neq 0\}$. Note that

$$\begin{aligned} & \underset{\beta}{\operatorname{argmin}} \min_{\alpha} \frac{1}{n} \sum_i W_i (T_i - (Y_i - \bar{Y})^\top \beta - (X_i - \bar{X})^\top \alpha)^2 \\ &= \underset{\beta}{\operatorname{argmin}} \frac{1}{n} \sum_i W_i (T_i - (\tilde{Y} - \bar{\tilde{Y}})^\top \beta)^2, \end{aligned}$$

where

$$\tilde{Y}_{ij} = Y_{ij} - X_i^\top \left[\left(\frac{1}{n} \sum_{i=1}^n W_i (X_i - \bar{X})(X_i - \bar{X})^\top \right)^{-1} \left(\frac{1}{n} \sum_{i=1}^n W_i (X_i - \bar{X})(Y_{ij} - \bar{Y}_j) \right) \right].$$

Therefore, our approach to include pre-treatment covariates closely resembles the adjustment of the CUPED estimator or Lin’s estimator. In particular, we adjust the outcomes Y with pre-treatment covariates using weighted linear regression.

Having identified \hat{S}_τ , using the second split, we compute the covariate-adjusted difference-in-means estimator such as the CUPED estimator or Lin’s estimator on \hat{S}_τ . The inference proceeds again as in Section 3 with covariates-adjusted \tilde{Y} restricted to the set \hat{S}_τ .

Our method shares a close relationship with the projection test (Lopes et al., 2011; Huang, 2015; Liu et al., 2022) in high-dimensional mean testing, as both involve finding sparse β using a quadratic objective function with ℓ_1 penalization. We focus on causal inference, and in particular as a result, we also consider pre-treatment covariates. Moreover, we employ a linear regression specification, making it easier for practitioners to implement our method with tools like `glmnet` in R (Friedman et al., 2010).

Algorithm 1 provides a summary of the proposed method.

Algorithm 1: Single-Split Algorithm

Input: $(T_i, X_i, Y_i)_{i=1}^n$

Output: \hat{S}_τ and the estimated treatment effects on \hat{S}_τ

- 1 Randomly split the data set into two folds $\mathcal{D}_1 = \{(T_i, X_i, Y_i)\}_{i=1}^{n_1}$ and $\mathcal{D}_2 = \{(T_i, X_i, Y_i)\}_{i=1}^{n_2}$
- 2 Using the first split \mathcal{D}_1 , estimate

$$\hat{S}_\tau = \{j | \hat{\beta}_j \neq 0\}$$

by fitting a weighted Lasso regression of T on centered Y and X as in (11).

- 3 Using the second split \mathcal{D}_2 , estimate the treatment effect $\hat{\tau}$ such that for $j \in \hat{S}_\tau$,

$$\hat{\tau}_j = \frac{1}{\sum_{i \in \mathcal{D}_2} T_i} \sum_{i \in \mathcal{D}_2} T_i \tilde{Y}_{ij}(1) - \frac{1}{\sum_{i \in \mathcal{D}_2} (1 - T_i)} \sum_{i \in \mathcal{D}_2} (1 - T_i) \tilde{Y}_{ij}(0),$$

where \tilde{Y}_j is defined as in (6) or (7), and estimate its variance $\hat{\Sigma}$ using (2) with \tilde{Y} on \hat{S}_τ .

Extension to Multi-Sample Splitting. Methods relying on sample splitting are known to be sensitive to the arbitrary choice of a one-time random split of the data (Meinshausen et al., 2008). Therefore, it is recommended to employ multiple splits and aggregate p-values from each split, as outlined in Meinshausen et al. (2008). This improves the robustness of the method by reducing the dependence on a single split. In Algorithm 2, we present an algorithm box where we apply the multi-sample splitting results from Meinshausen et al. (2008) to our proposed method. Note that one consequence of using multiple splits is that while we obtain an aggregated p-value for testing the null hypothesis, we no longer obtain an estimated subset localizing the treatment effect (since each split produces one such subset). Aggregating the subsets remains an interesting direction for future work.

In the remainder of the section we first discuss the reduction of (8) to a weighted least squares regression; and then present a result that provides conditions under which we recover S_τ .

5.1 Reduction to Weighted Linear Regression

Consider the following weighted least squares regression problem:

$$\hat{\beta} = \arg \min_{\beta} \frac{1}{n} \sum_i W_i (T_i - (Y_i - \bar{Y})^\top \beta)^2.$$

We set the weights so that the least-squares problem becomes equivalent to a *signal strength maximization* problem, where the signal strength is defined using Hotelling T^2 statistic in (3).

Algorithm 2: Multi-Split Algorithm

Input: $(T_i, X_i, Y_i)_{i=1}^n, \gamma$

Output: valid p-values under $H_0 : \tau = 0$

1 **for** $b = 1, \dots, B$ **do**

2 Perform Algorithm 1. We have $\hat{S}_\tau^{(b)}$ from the first split and the treatment effect estimate $\hat{\tau}^{(b)}$ restricted to the set $\hat{S}_\tau^{(b)}$ and its variance estimate $\hat{\Sigma}^{(b)}$ from the second split.

3 Calculate p-value:

(a) (P-values with multiple testing) The p-value for each Y_j is

$$p_j^{(b)} = \left(1 - \Phi\left(|\hat{\tau}_j^{(b)}|/\sqrt{n\hat{\Sigma}_{jj}^{(b)}}\right)\right) \cdot |\hat{S}_\tau^{(b)}| \quad \text{for } j \in \hat{S}_\tau^{(b)}$$

$$p_j^{(b)} = 1 \quad \text{for } j \notin \hat{S}_\tau^{(b)},$$

where Φ is the cdf of the standard Gaussian distribution.

(b) (P-value with Hotelling T^2 statistic) The p-value is

$$p_1^{(b)} = P\left(\chi^2\left(|\hat{S}_\tau^{(b)}|\right) \geq n_2 \hat{\tau}^{(b)\top} (\hat{\Sigma}^{(b)})^{-1} \hat{\tau}^{(b)}\right),$$

where $\chi^2(df)$ follows the chi-squared distribution with the degree of freedom df .

4 Aggregate p-values as

$$P_j(\gamma) = \min\left[1, q_\gamma\left(\{p_j^{(b)}/\gamma; b = 1, \dots, B\}\right)\right],$$

where $q_\gamma(\cdot)$ is the (empirical) γ -quantile function.

We define Y^S to be an outcome vector restricted to the set S as $Y^S := (Y_j | j \in S)^\top$.

To start, consider the unweighted setting. Here, the residual sum of squares (RSS) of the linear regression is

$$\begin{aligned} \frac{1}{n} \sum_i (T_i - (Y_i^S - \bar{Y}^S)^\top \hat{\beta})^2 &= C_1 - C_2 \cdot \hat{\tau}_{\text{DiM}}^S{}^\top \left(\hat{\Sigma}^S + C_3 \cdot \hat{\tau}_{\text{DiM}}^S \hat{\tau}_{\text{DiM}}^S{}^\top \right)^{-1} \hat{\tau}_{\text{DiM}}^S \\ &= C_1 - C_2 \cdot \frac{\hat{\tau}_{\text{DiM}}^S{}^\top (\hat{\Sigma}^S)^{-1} \hat{\tau}_{\text{DiM}}^S}{1 + C_3 \cdot \hat{\tau}_{\text{DiM}}^S{}^\top (\hat{\Sigma}^S)^{-1} \hat{\tau}_{\text{DiM}}^S} \end{aligned} \quad (12)$$

by applying the Sherman–Morrison formula. Note that $C_1, C_2, C_3 > 0$. Details can be found in the Appendix, Section A. The $\hat{\tau}_{\text{DiM}}^S$ is defined as in (1) (restricted to the subset S) and $\hat{\Sigma}^S$ is defined as

$$\begin{aligned} \hat{\Sigma}^S &= \frac{n}{n_c} \cdot \frac{1}{n_t} \sum_i T_i (Y_i^S(1) - \bar{Y}^S(1)) (Y_i^S(1) - \bar{Y}^S(1))^\top \\ &\quad + \frac{n}{n_t} \cdot \frac{1}{n_c} \sum_i (1 - T_i) (Y_i^S(0) - \bar{Y}^S(0)) (Y_i^S(0) - \bar{Y}^S(0))^\top. \end{aligned} \quad (13)$$

We want to correct $\hat{\Sigma}^S$ by introducing weights W_i so that $\hat{\Sigma}^S$ becomes $\hat{\Sigma}_{\text{DiM}}^S$.

We design the following weights:

$$W_i = \frac{1}{\hat{\pi}^2} T_i + \frac{1}{(1 - \hat{\pi})^2} (1 - T_i),$$

where $\hat{\pi} = \sum_i T_i/n$. Under these weights, the RSS of the weighted linear regression is now

$$\sum_i W_i (T_i - (Y_i^S - \bar{Y}^S)^\top \hat{\beta})^2 = C_1 - C_2 \cdot \frac{\hat{\tau}_{\text{DiM}}^S{}^\top (\hat{\Sigma}_{\text{DiM}}^S)^{-1} \hat{\tau}_{\text{DiM}}^S}{1 + \left(\frac{n_c}{n_t} + \frac{n_t}{n_c} - 1\right) \cdot \hat{\tau}_{\text{DiM}}^S{}^\top (\hat{\Sigma}_{\text{DiM}}^S)^{-1} \hat{\tau}_{\text{DiM}}^S}, \quad (14)$$

where $C_1, C_2 > 0$. Details can be found in the Appendix, Section A.

In (14), C_1, C_2, C_3 do not depend on the given set S but $\hat{\tau}_{\text{DiM}}^S$ and $\hat{\Sigma}_{\text{DiM}}^S$ do. This indicates that for any $s \leq p$, for a subset of outcomes S such that $|S| = s$, we have

$$\min_{S: |S|=s} \text{RSS of weighted linear regression with } Y^S = \max_{S: |S|=s} \hat{\tau}_{\text{DiM}}^S \mathbf{r}^{\top} (\hat{\Sigma}_{\text{DiM}}^S)^{-1} \hat{\tau}_{\text{DiM}}^S.$$

On the right-hand side, $\hat{\tau}_{\text{DiM}}^S$ and $\hat{\Sigma}_{\text{DiM}}^S$ are obtained for each S . Note that the right-hand side is a Hotelling T^2 statistic in (3). This means that with our chosen weights, the weighted least-squares problem becomes equivalent to maximization of the Hotelling T^2 statistic, as desired.

5.2 Recovery Results for the Lasso

In this section, we provide theoretical results for our approach using the LASSO. In particular, we state the assumptions under which our proposed method can consistently recover S_τ , and provide the error bound for any optimal solution of (11).

Recall that $\hat{\beta}$ is defined as

$$(\hat{\beta}, \hat{\alpha}) = \underset{\beta \in \mathbb{R}^p, \alpha \in \mathbb{R}^m}{\operatorname{argmin}} \frac{1}{n} \sum_i W_i (T_i - (Y_i - \bar{Y})^\top \beta - (X_i - \bar{X})^\top \alpha)^2 + 2\lambda_n \|\beta\|_1$$

where $\lambda_n > 0$ is a user-defined regularization penalty.

Define the (population-level) covariate-adjusted potential outcomes Z as

$$Z := Y - (1 - \pi) \cdot [\text{Var}(X)^{-1} \text{Cov}(X, Y(1))]^\top X - \pi \cdot [\text{Var}(X)^{-1} \text{Cov}(X, Y(0))]^\top X.$$

Note that this adjustment of outcomes Y on pre-treatment covariates X resembles pre-treatment covariates adjustments with linear regressions in Lin (2013) and Jin and Ba (2023). If pre-treatment covariates are not available, set $Z = Y$.

We will provide the error bound for $\|\hat{\beta} - \beta^*\|_1$, where the optimal solution of the population risk β^* is defined as

$$\beta^* = \frac{1 - \pi}{\pi} \left(\Sigma_Z + \left(\frac{1 - \pi}{\pi} + \frac{\pi}{1 - \pi} - 1 \right) \tau \tau^\top \right)^{-1} \tau.$$

where

$$\begin{aligned} \tau &:= \mathbb{E}[Z(1) - Z(0)] = \mathbb{E}[Y(1) - Y(0)], \\ \Sigma_Z &:= \frac{1}{\pi} \text{Var}(Z(1)) + \frac{1}{1 - \pi} \text{Var}(Z(0)). \end{aligned}$$

By Sherman-Morrison formula,

$$\beta^* \propto \Sigma_Z^{-1} \tau.$$

In our setting in Section 3, the treatment effect τ is sparse, with only s_τ nonzero elements. In the following, we assume that β^* is sparse, with only s^* nonzero elements. This is assuming that the inverse of Σ_Z is sparse. Below, we provide examples where the inverse of Σ_Z and thus β^* are sparse under an appropriate structural causal model (Bollen, 1989; Pearl, 2009). Let $S^* = \{j | \beta_j^* \neq 0\}$. In examples below, we identify setting where $S_\tau \subseteq S^*$. Note that for the remainder of this section, we present the recovery results for S^* , which would include S_τ in settings below. We also provide simulation results when the sparsity assumption is slightly violated in the Appendix C.

Assumption 1 (Sparsity). β^* is sparse with only s^* nonzero elements.

Example 1. Consider the linear structural causal model:

$$Y = \alpha_0 + \Theta_0 X + T \cdot (\alpha_1 + \Theta_1 X) + \epsilon,$$

where $\alpha_0, \alpha_1 \in \mathbb{R}^p$, $\Theta_0, \Theta_1 \in \mathbb{R}^{p \times m}$, and $X \perp \epsilon$. Suppose that the treatment effect is sparse; there exists S_τ such that for $j \notin S_\tau$, we have $\alpha_{1j} = 0$ and the j -th row $\Theta_1^j = \mathbf{0}$.

Assume that $\epsilon_1, \dots, \epsilon_p$ are mean zero and uncorrelated with each other. Then, we have

$$S_\tau := \{j : \tau_j \neq 0\} = S^* := \{j : \beta_j^* \neq 0\}.$$

Example 2. In this example we consider the same linear structural causal model as in the previous example, but instead of assuming that $\epsilon_1, \dots, \epsilon_p$ are uncorrelated with each other, we assume a cluster structure: there exist clusters C_1, \dots, C_c such that if $j \in C_i$ and $j' \in C_{i'}$ with $i \neq i'$, then ϵ_j and $\epsilon_{j'}$ are uncorrelated. Then, when $S_\tau \subseteq C_1$, we have

$$S_\tau \subseteq S^* = C_1.$$

With a sparse cluster structure, $s^* = |C_1| \ll p$.

Example 3. Continue to assume the same linear structural causal model, but now assume that ϵ follows a multivariate normal distribution and “most” variables are conditionally independent of each other given the remaining variables. For example, we could consider an autoregressive model ($AR(k)$) for time-series data. Then, the inverse covariance matrix of ϵ is sparse, and we have

$$S_\tau \subseteq S^* = \text{Markov Blanket of } S_\tau \text{ under the graph of } \epsilon.$$

With a sparsely connected graph structure of ϵ , $s^* \ll p$.

For our theoretical results, we assume sub-Gaussian designs for X , $Y(0)$, $Y(1)$, and thus for $Z(0)$, $Z(1)$ as well. Then, we add assumptions about their moments and the invertibility of the covariance matrix of X .

Assumption 2 (Sub-Gaussian Designs). X_1, \dots, X_n are independent and identically distributed sub-Gaussian vectors with mean μ_X and covariance Σ_X . Moreover, $Y_1(0), \dots, Y_n(0)$ and $Y_1(1), \dots, Y_n(1)$ are independent and identically distributed sub-Gaussian vectors with mean μ_Y^0 and μ_Y^1 respectively and covariance Σ_Y^0 and Σ_Y^1 respectively. Additionally, $Z_1(0), \dots, Z_n(0)$ and $Z_1(1), \dots, Z_n(1)$ are independent and identically distributed sub-Gaussian vectors. Let the mean be μ_Z^0 and μ_Z^1 respectively and the covariance be Σ_Z^0 and Σ_Z^1 respectively. More specifically, each variable $(Z(0))_j / \sqrt{(\Sigma_Z^0)_{jj}}$ is sub-Gaussian with parameter σ_Z^0 and $(Z(1))_j / \sqrt{(\Sigma_Z^1)_{jj}}$ is sub-Gaussian with parameter σ_Z^1 for $j = 1, \dots, p$.

Assumption 3 (Moments). The first and second moments of $X, Y(0), Y(1), Z(0), Z(1)$ are bounded.

Assumption 4 (Invertibility of Σ_X). The minimum eigenvalue of Σ_X is bounded away from zero.

A crucial assumption in the proof of the oracle inequalities for Lasso is the *restricted eigenvalue* (RE) condition introduced by [Bickel et al. \(2009\)](#) for the covariance matrix. When $p > n$, the sample covariance matrix is not positive definite. RE conditions imply a kind of restricted positive definiteness. Let $J(\beta) = \{j \in \{1, \dots, p\} : \beta_j \neq 0\}$. For a vector $\delta \in \mathbb{R}^p$ and a subset $J \subset \{1, \dots, p\}$, we denote by δ_J the vector in \mathbb{R}^p that has the same coordinates as δ on J and zero coordinates on the complement J^c of J . We say that Σ satisfies the $\text{RE}(s, c_0, \Sigma)$ condition with parameter $\kappa(s, c_0, \Sigma)$ if

$$\kappa(s, c_0, \Sigma) = \min_{\substack{J_0 \subseteq \{1, \dots, p\} \\ |J_0| \leq s}} \min_{\substack{\delta \in \mathbb{R}^p, \delta \neq 0, \\ \|\delta_{J_0^c}\| \leq c_0 \|\delta_{J_0}\|_1}} \frac{\delta^\top \Sigma \delta}{\|\delta_{J_0}\|_2^2} > 0.$$

Several sufficient conditions for RE conditions can be found in [Bickel et al. \(2009\)](#).

In Assumption 5, we assume appropriate RE conditions as well as additional sparse eigenvalue conditions for population covariance matrices of Z , Σ_Z^0 and Σ_Z^1 . Essentially, this suggests that the covariance matrix of outcomes, after (population-level) linear covariates adjustment, satisfies some *restricted* positive definiteness.

Assumption 5 (RE condition). Σ_Z^0 satisfies $\text{RE}(s^*, 3, \Sigma_Z^0)$ condition with parameter $\kappa(s^*, 3, \Sigma_Z^0)$ and Σ_Z^1 satisfies $\text{RE}(s^*, 3, \Sigma_Z^1)$ condition with parameter $\kappa(s^*, 3, \Sigma_Z^1)$. Furthermore, the maximum s^* -sparse eigenvalues for both groups are bounded, which means that for some constant $\rho > 0$,

$$\max_{\|\delta\|_2=1, \|\delta\|_0 \leq s^*} \delta^\top \Sigma_Z^0 \delta, \quad \max_{\|\delta\|_2=1, \|\delta\|_0 \leq s^*} \delta^\top \Sigma_Z^1 \delta \leq \rho.$$

Finally, we assume that the optimal solution β^* is well-behaved, with $\|\beta^*\|_1$ bounded.

Assumption 6 (Bounded $\|\beta^*\|_1$). $\|\beta^*\|_1$ is bounded by $M > 0$.

In the following theorem, we first establish the error bound for $\|\hat{\beta} - \beta^*\|_1$, and show that we can recover S^* consistently with the hard-threshold Lasso estimator. The proof largely follows the proof of Theorem 7.2 in [Bickel et al. \(2009\)](#), and can be found in the Appendix, Section B. Note that we allow the dimension of outcome representations to be $p \gg n$, but we assume that the dimension of pre-treatment covariates m is fixed.

Theorem 1 (Rate and Recovery). *Suppose assumptions stated above hold and $\min(n_t/n, n_c/n) \geq r > 0$. Consider $\hat{\beta}$ defined in (11) with $\lambda_n \geq A\sqrt{\log p/n}$ for some sufficiently large $A > 0$. Then, for sufficiently large $n \gg s^* \log p$, we have*

$$\|\hat{\beta} - \beta^*\|_1 \leq \text{Const } s^* \lambda_n,$$

with probability at least $1 - c_1 \exp(-c_2 n \lambda_n^2)$ for some constants $\text{Const}, c_1, c_2 > 0$. Further, if

$$\min_{j \in S^*} |\beta_j^*| \gg \text{Const } s^* \lambda_n \quad \text{as } n \rightarrow \infty,$$

and \hat{S}^* is defined using the hard-threshold Lasso estimator as

$$\hat{S}^* = \{j \mid |\hat{\beta}_j| > \text{Const } s^* \lambda_n\},$$

then we have a consistent recovery of S^* as $\mathbb{P}(\hat{S}^* = S^*) \rightarrow 1$ as $n \rightarrow \infty$.

Remark 1. Note that $s^* \lambda_n = o(1)$ implies $s^* \ll \sqrt{n}$. Consider the classical setting, where the number of samples n goes to infinity, but the sparsity index s^* do not depend on n . One could choose $\lambda_n^2 = 1/n^{1-\delta}$ for some $\delta > 0$. Then with probability greater than $1 - \tilde{c}_1 \exp(-\tilde{c}_2 n^\delta)$, which converges to 1 as $n \rightarrow \infty$, we have an error bound for $\|\hat{\beta} - \beta^*\|_1$ that converges to 0.

6 Numerical Experiments

6.1 Simulations

We compare the performance of the baseline and the proposed methods with pre-treatment covariates adjustment, as presented in Section 5, through a simulation study. In scenarios where the data generation process involves independent outcomes and a constant treatment effect without pre-treatment covariates, both the baseline and proposed approaches demonstrate similar performance. Additional details can be found in the Appendix C. However, in a more realistic and complicated setting as follows, our proposed method outperforms the baseline method in most cases.

We generate data as follows. First, we randomly sample the model parameters as

$$\begin{aligned} \beta_j &= (U_{j1}, \dots, U_{jm}) \quad \text{where } U_{j1}, \dots, U_{jm} \stackrel{i.i.d.}{\sim} \text{Unif}(-1, 1) \\ \delta_j &= (U'_{j1}, \dots, U'_{jm}) \quad \text{where } U'_{j1}, \dots, U'_{jm} \stackrel{i.i.d.}{\sim} \text{Unif}(0, 1) \end{aligned}$$

for $j = 1, \dots, p$, where p is the outcome dimension. Next, for the generated model parameters β and δ , we randomly generate n samples in the following manner:

$$\begin{aligned} Y_{ij} &= X_i^\top \beta_j + T_i \cdot (\alpha + X_i^\top \delta_j) \cdot I(j \leq s_\tau) + \epsilon_{ij}, \\ X_i &\stackrel{i.i.d.}{\sim} N(0, I_{m \times m}), \quad T_i \stackrel{i.i.d.}{\sim} \text{Bernoulli}(\pi), \quad \epsilon_{ij} \stackrel{i.i.d.}{\sim} N(0, 1), \end{aligned}$$

for $i = 1, \dots, n$ and $j = 1, \dots, p$. Note that there are non-zero treatment effects on $S_\tau = \{Y_1, \dots, Y_{s_\tau}\}$, where s_τ is a pre-specified sparsity index in the simulation process.

We evaluate the performance of the proposed method relative to the baseline method, both with adjustment for pre-treatment covariates, based on how well the ranking recovers S_τ . The ranking is obtained as follows: For the baseline method, individual outcome dimensions are ranked based on their treatment effect sizes. For the proposed method, we consider regularization paths for a fine grid of λ values and track a corresponding sequence of active sets (the set with non-zero coefficients)

of increasing size. The ranking is determined by the order in which outcome dimensions enter the Lasso path. The *recovery rate* is defined as follows: For a given s , denote $S(s)$ as the selected subset of outcome dimensions of size s obtained from applying each method with pre-treatment covariates adjustment. Then, for each method, the recovery rate of S_τ is $|S(s) \cap S_\tau|/s$ for $1 \leq s \leq s_\tau$.

The recovery rates comparing the proposed to baseline approaches (with pre-treatment covariates adjustment) for different sample sizes (n), probabilities of being treated (π), and magnitudes of treatment effects (α) are given in Figure 3. We set the outcome dimension $p = 100$, the number of pre-treatment covariates $m = 30$, and the sparsity index $s_\tau = 5$. Note that in simulations, we use the elastic net penalty (Zou and Hastie, 2005) instead of the Lasso penalty as the elastic net is known to encourage a grouping effect: correlated predictors tend to be in or out of the model together. We see that our proposed method outperforms baseline methods in most scenarios, especially when sample sizes are small and signals are weak. When sample sizes and signals are large, the proposed method tends to identify a subset of S_τ more quickly than baseline methods, but performs slightly worse in discovering the full S_τ .

6.2 Semi-Synthetic Data

In this section, we demonstrate the performance of our method using semi-synthetic data motivated from the time series data example introduced in Section 1. Following the protocol discussed in Section 1, we curate a dataset with $n = 5,000$ samples of the average 24-hour period for a week of real CGM data before and after a potential treatment. For each sample i , let the transformed glucose traces be $\text{glucose}_i \in \mathbb{R}^{288 \times 2=576}$, where 288 represents 24 hours of data recorded at 5 minute intervals averaged over the 7 days in a given week and we concatenate this 24-hour period average representation for Week 1 and Week 2. An example of such a transformed CGM trace is illustrated in Figure 1.

Generalizing the procedure of Section 1, we generate semi-synthetic data by simulating a treatment effect that occurs within a random two-hour time interval of the day. For example, the treatment effect might occur following lunch, between 12pm and 2pm. Given a randomly selected two-hour interval I in which the treatment effect may manifest, a synthetic constant treatment effect of magnitude α is applied as

$$\text{glucose}_{it} = \text{glucose}_{it} - \alpha,$$

if sample i is treated and $t \in I$. As before, we randomize treatment assignment with probability of 0.5 of a sample receiving a treatment.

Suppose the scientist is uncertain about the location and duration of the treatment effect. One approach they might consider is as follows. First, they might examine the time-in-range (TIR) in 6 four-hour windows, each roughly corresponding to *early morning*, *late morning*, *afternoon*, *evening*, *night*, and *overnight*. They may then decide they prefer a more refined representation and consider TIR in 12 two-hour windows. Suppose in each scenario the scientist compares the differences in TIR before and after the treatment for each window and conducts multiple testing. As previously discussed in Section 1, if the actual treatment duration is more localized than the window size under consideration, as in the first scenario considering 4-hour windows, it is highly likely that the treatment signal will be lost. The second representation happens to be a fortuitous selection as the actual duration of the simulated treatment effect is two hours; however, as we illustrate in Figure 4, our proposed method still outperforms the default multiple testing approach the scientist would employ.

In contrast to using pre-defined windows, our proposed approach allows for exploration of more refined windows while achieving superior power. In the first stage, we randomly partition the data set into two splits. Within the first split, we aim to locate the treatment effect and consider multiple resolutions for the representation. We denote 6 four-hour windows as *level 0*, 12 two-hour windows as *level 1*, and 24 one-hour windows as *level 2*. We perform subset selection with our proposed method where we set the pre-treatment covariates X to be TIR of considered windows of the pre-treatment week (Week 1) and Y to be TIR of considered windows of the post-treatment week (Week 2). We perform subset selection for each level and compute the RSS for the selected subset within the level. The level and corresponding selected subset with the smallest RSS is chosen. Moving to the second split, we estimate the treatment effect utilizing the selected subset of the chosen level. We apply the multi-sample splitting procedure of Meinshausen et al. (2008) to our entire process to reduce the

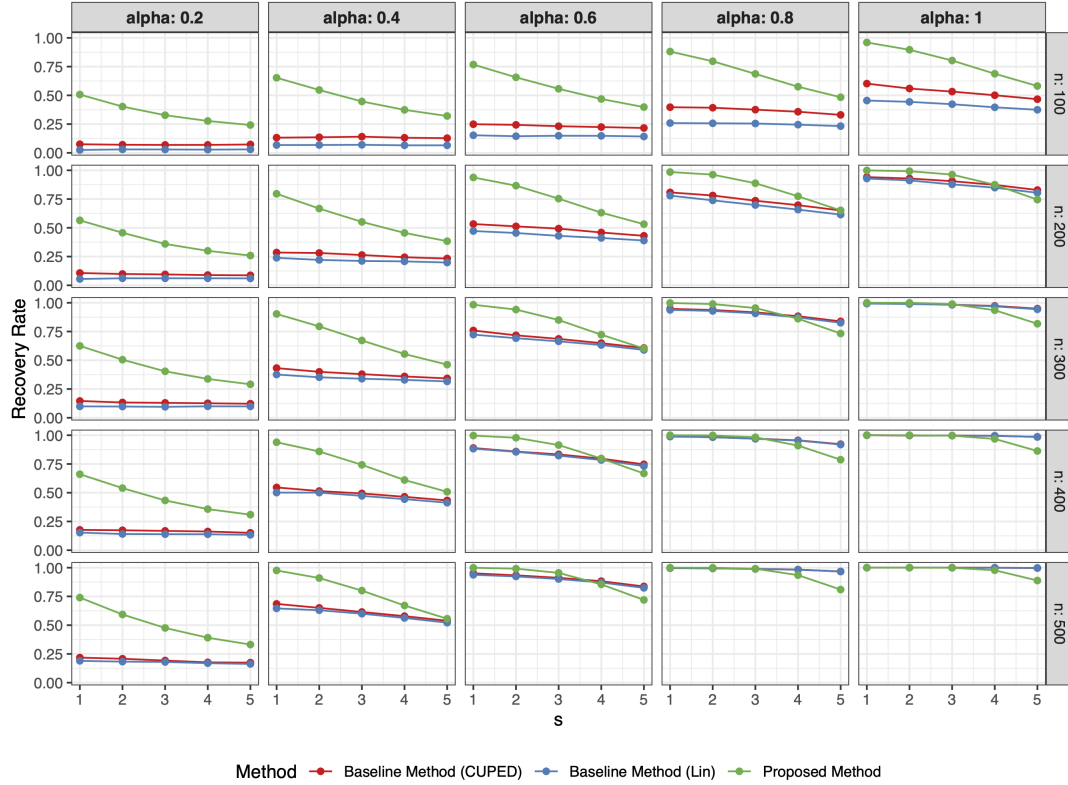
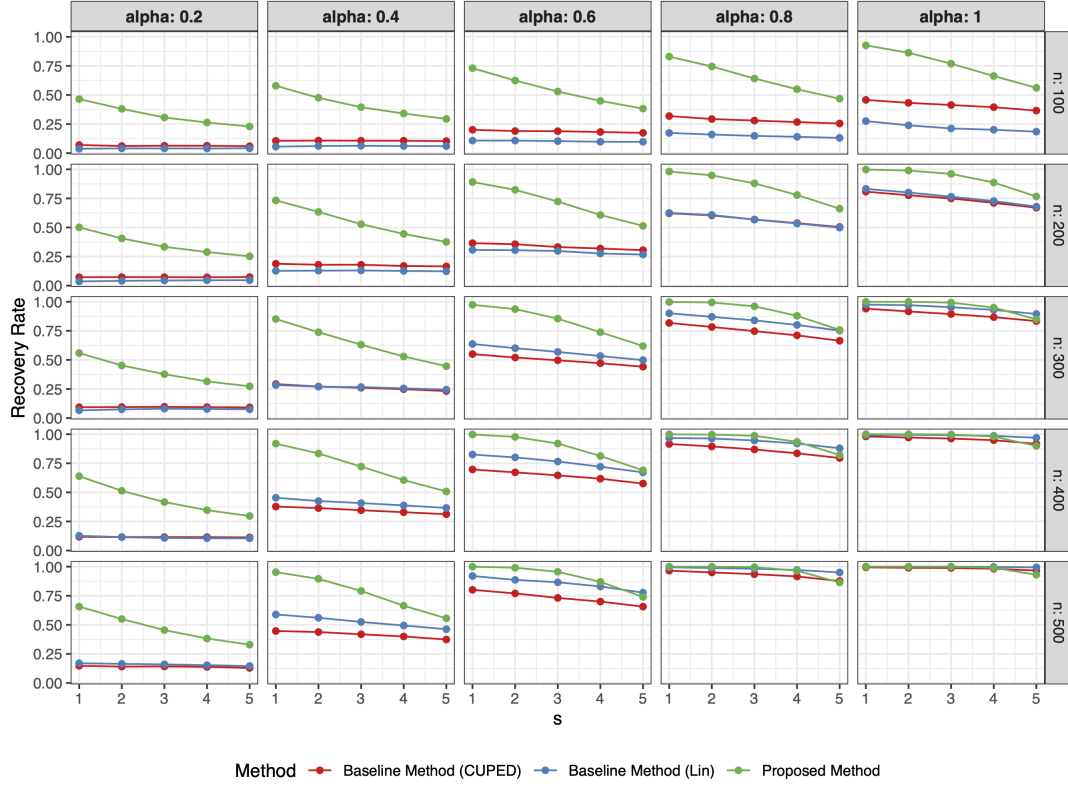


Figure 3: Recovery rates averaged over 1000 replicates for the baseline and proposed approaches with pre-treatment covariates adjustment for $n = 100, 200, 300, 400, 500$ and $\alpha = 0.2, 0.4, 0.6, 0.8$ for $\pi = 0.3$ (Above) and $\pi = 0.5$ (Below).

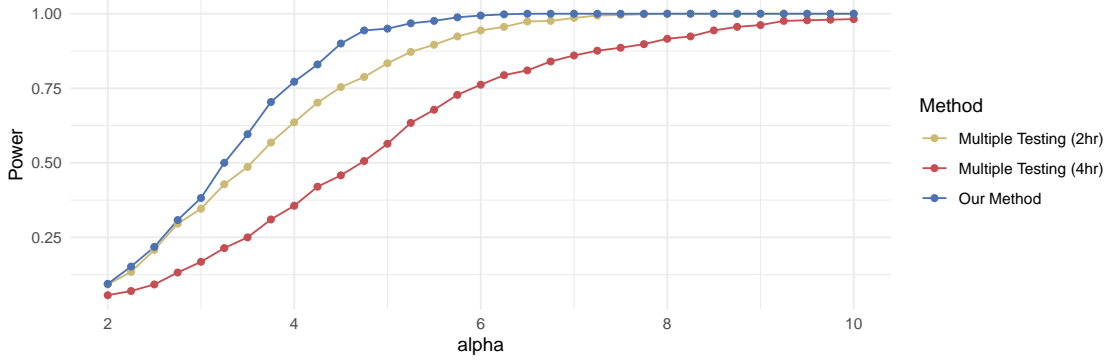


Figure 4: Power plots for the semi-synthetic glucose data comparing our proposed method (blue) to a default method of looking at a pre-specified representation of 4-hour windows (red) or 2-hour windows (yellow) and then applying multiple testing.

dependence on the random data split; see Algorithm 2.

The entire process, involving the generation of a random two-hour treatment effect and the application of methods introduced above, is repeated 1000 times. The powers of the considered methods from these 1000 iterations are presented in Figure 4. We see that our method achieves better power than the default method of using pre-specified representations and multiple testing.

7 Discussion

This paper addresses the problem of causal inference from experimental data with high-dimensional outcomes. Our emphasis is on the development of a practical, easily deployed method that can identify the sparse subset of outcome representations most likely to contain the treatment effect given a large pool of outcome representations. We introduce a sparse regression approach for subset selection, where we employ a ℓ_1 -regularized weighted linear regression with carefully chosen weights. We provide theoretical results showing that our method can recover the subset of outcome representations consistently. In simulated and semi-synthetic experiments, we empirically demonstrate that our method outperforms the baseline methods, especially when the signal-to-noise ratio is relatively weak.

Looking ahead, a key challenge lies in the sample-splitting framework. Multiple correction testing may experience decreased power due to a potentially large correction factor. However, methods based on sample splitting may suffer from reduced power as they utilize only half of the data for treatment effect estimation. Compared to the baseline (individual ranking based) subset selection method, our method performs better in low sample-size settings, suggesting the potential for allocating more samples to the second data split for the actual treatment effect estimation. Nonetheless, the overall process necessitates sufficient sample sizes. There are many real-world examples where the primary challenge is obtaining adequate sample sizes. For those cases, alternative approaches beyond sample splitting may be required. However, there are also many scenarios where sample sizes are sufficient, but the size of the treatment effect is small; our procedures is particularly well-suited to such scenarios. More generally, in the setting where scientists believe the treatment effect is sparse and are interested in selecting the outcome representations in which the treatment effect potentially manifests, our approach provides practical guidance on how to do so.

8 Acknowledgement

The authors would like to thank Kevin Guo, James Yang, Samir Khan, Yu Wang, and Tim Morrison for their insightful comments and helpful feedback. The authors would also like to thank Johannes Ferstad for assistance with the data set used in the experiments above.

References

- G. Aleppo, K. J. Ruedy, T. D. Riddlesworth, D. F. Kruger, A. L. Peters, I. B. Hirsch, R. M. Bergenstal, E. Toschi, A. J. Ahmann, V. N. Shah, M. R. Rickels, B. W. Bode, A. Philis-Tsimikas, R. Pop-Busui, H. Rodriguez, E. Eyth, A. Bhargava, C. Kollman, and R. W. R.-B. S. G. Beck. Replace-bg: A randomized trial comparing continuous glucose monitoring with and without routine blood glucose monitoring in adults with well-controlled type 1 diabetes. *Diabetes Care*, 40(4):538–545, 2017.
- A. Anand, Y. Li, Y. Wang, J. Wu, S. Gao, L. Bukhari, V. Mathews, A. Kalnin, and M. Lowe. Antidepressant effect on connectivity of the mood-regulating circuit: an fmri study. *Neuropsychopharmacology*, 30(7):1334–1344, 2005.
- Y. Bengio, A. Courville, and P. Vincent. Representation learning: A review and new perspectives. *IEEE transactions on pattern analysis and machine intelligence*, 35:1798–1828, 2013.
- P. J. Bickel, Y. Ritov, and A. B. Tsybakov. Simultaneous analysis of lasso and dantzig selector. *The Annals of Statistics*, 37(4):1705 – 1732, 2009.
- A. Bloniarz, H. Liu, C.-H. Zhang, J. S. Sekhon, and B. Yu. Lasso adjustments of treatment effect estimates in randomized experiments. *Proceedings of the National Academy of Sciences*, 113(27):7383–7390, 2016.
- K. Bollen. *Structural Equations with latent variables*. John Wiley & Sons, 1989.
- F. Bunea, A. B. Tsybakov, and M. H. Wegkamp. Sparsity oracle inequalities for the lasso. *Electronic Journal of Statistics*, 1:169–194, 2007.
- A. Deng, Y. Xu, R. Kohavi, and T. Walker. Improving the sensitivity of online controlled experiments by utilizing pre-experiment data. In *Proceedings of the sixth ACM international conference on Web search and data mining*, 2013.
- J. Friedman, R. Tibshirani, and T. Hastie. Regularization paths for generalized linear models via coordinate descent. *Journal of Statistical Software*, 33(1):1–22, 2010.
- T. Hastie, R. Tibshirani, and R. Tibshirani. Best subset, forward stepwise or lasso? analysis and recommendations based on extensive comparisons. *Statistical Science*, 35(4):579–592, 2020.
- Y. Huang. Projection test for high-dimensional mean vectors with optimal direction. *Department of Statistics, The Pennsylvania State University at University Park*, 2015.
- Y. Huang, C. Li, R. Li, and S. Yang. An overview of tests on high-dimensional means. *Journal of Multivariate Analysis*, 188, 2022.
- G. Imbens and D. Rubin. *Causal inference in statistics, social, and biomedical sciences*. Cambridge University Press, 2015.
- Y. Jin and S. Ba. Toward optimal variance reduction in online controlled experiments. *Technometrics*, 65(2):231–242, 2023.
- A. Koenig, D. Mechanic-Hamilton, S. Xie, M. Combs, A. Cappola, L. Xie, J. Detre, D. Wolk, and S. Arnold. Effects of the insulin sensitizer metformin in alzheimer disease: Pilot data from a randomized placebo-controlled crossover study. *Alzheimer Dis Assoc Disord*, 31(2):107–113, 2017.
- W. Lin. Agnostic notes on regression adjustments to experimental data: Reexamining freedman’s critique. *The Annals of Applied Statistics*, 7(1):295–318, 2013.
- W. Liu, X. Yu, and R. Li. Multiple-splitting projection test for high-dimensional mean vectors. *Journal of Machine Learning Research*, 23, 2022.
- M. Lopes, L. Jacob, and M. J. Wainwright. A more powerful two-sample test in high dimensions using random projection. In *Advances in Neural Information Processing Systems*, pages 1206–1214, 2011.
- K. Lounici. Sup-norm convergence rate and sign concentration property of lasso and dantzig selector. *Electronic Journal of Statistics*, 2:90–102, 2008.

- N. Meinshausen and P. Bühlmann. High-dimensional graphs and variable selection with the lasso. *The Annals of Statistics*, 34(3):1436–1462, 2006.
- N. Meinshausen and B. Yu. Lasso-type recovery of sparse representations for high-dimensional data. *The Annals of Statistics*, 37(1):246–270, 2009.
- N. Meinshausen, L. Meier, and P. Bühlmann. P-values for high-dimensional regression. *Journal of the American Statistical Association*, 104(488), 2008.
- S. N. Negahban, P. Ravikumar, M. J. Wainwright, and B. Yu. A unified framework for high-dimensional analysis of m -estimators with decomposable regularizers. *Advanced in Neural Information Processing Systems*, 2009.
- J. Pearl. *Causality: Models, reasoning, and inference*. Cambridge University Press, 2nd edition, 2009.
- P. Ravikumar, M. J. Wainwright, G. Raskutti, and B. Yu. High-dimensional covariance estimation by minimizing ℓ_1 penalized log-determinant divergence. *Electronic Journal of Statistics*, 5(none), 2011.
- R. Tibshirani. Regression shrinkage and selection via the lasso. *Journal of the Royal Statistical Society. Series B (Methodological)*, 58(1):267–288, 1996.
- S. A. van de Geer. High-dimensional generalized linear models and the lasso. *The Annals of Statistics*, 36(2):614–645, 2008.
- S. Wager, W. Du, J. Taylor, and R. J. Tibshirani. High-dimensional regression adjustments in randomized experiments. *Proceedings of the National Academy of Sciences*, 115(10):2602–2607, 2018.
- M. J. Wainwright. Sharp thresholds for high-dimensional and noisy sparsity recovery using ℓ_1 -constrained quadratic programming (lasso). *IEEE Transactions on Information Theory*, 55(5):2183–2202, 2009.
- M. J. Wainwright. *High-Dimensional Statistics: A Non-Asymptotic Viewpoint*. Cambridge Series in Statistical and Probabilistic Mathematics. Cambridge University Press, 2019.
- L. Wasserman and K. Roeder. High-dimensional variable selection. *The Annals of Statistics*, 37(5A):2178–2201, 2009.
- T. Zhang and H. Huang. Sparsity and the lasso. *IEEE Transactions on Information Theory*, 57(1):468–487, 2008.
- P. Zhao and B. Yu. On model selection consistency of lasso. *The Journal of Machine Learning Research*, 7:2541–2563, 2006.
- S. Zhou. Restricted eigenvalue conditions on subgaussian random matrices. Available at <http://arxiv.org/pdf/0912.4045v2.pdf>, 2009.
- H. Zou and T. Hastie. Regularization and variable selection via the elastic net. *Journal of the Royal Statistical Society Series B: Statistical Methodology*, 67(2):301–320, 2005.

Appendix

Section A contains calculations for Section 5.1 and Section B contains the proofs for Section 5.2.

A Calculations for Section 5.1

Let us first show the equation (12). Note that

$$\begin{aligned} & \sum_i (T_i - (Y_i^S - \bar{Y}^S)^\top \hat{\beta})^2 \\ &= \sum T_i - \sum T_i (Y_i^S - \bar{Y}^S)^\top \left(\sum (Y_i^S - \bar{Y}^S)(Y_i^S - \bar{Y}^S)^\top \right)^{-1} \sum T_i (Y_i^S - \bar{Y}^S). \end{aligned}$$

We have that

$$\begin{aligned} \sum T_i (Y_i^S - \bar{Y}^S) &= \sum T_i Y_i^S - \bar{Y}^S \sum T_i \\ &= \sum T_i Y_i^S(1) - \frac{n_t}{n} \left(\sum T_i Y_i^S(1) + \sum (1 - T_i) Y_i^S(0) \right) \\ &= \frac{n_t n_c}{n} \left(\frac{1}{n_t} \sum T_i Y_i^S(1) - \frac{1}{n_c} \sum (1 - T_i) Y_i^S(0) \right). \end{aligned}$$

Moreover, we get that

$$\begin{aligned} & \frac{1}{n} \sum (Y_i^S - \bar{Y}^S)(Y_i^S - \bar{Y}^S)^\top = \frac{1}{n} \sum Y_i^S Y_i^{S\top} - \bar{Y}^S \bar{Y}^{S\top} \\ &= \frac{1}{n} \sum T_i Y_i^S(1) Y_i^S(1)^\top + \frac{1}{n} \sum (1 - T_i) Y_i^S(0) Y_i^S(0)^\top - \bar{Y}^S \bar{Y}^{S\top} \\ &= \frac{n_t}{n} \left(\frac{1}{n_t} \sum T_i Y_i^S(1) Y_i^S(1)^\top - \left(\frac{1}{n_t} \sum T_i Y_i^S(1) \right) \left(\frac{1}{n_t} \sum T_i Y_i^S(1) \right)^\top \right) \\ &+ \frac{n_c}{n} \left(\frac{1}{n_c} \sum (1 - T_i) Y_i^S(0) Y_i^S(0)^\top - \left(\frac{1}{n_c} \sum (1 - T_i) Y_i^S(0) \right) \left(\frac{1}{n_c} \sum (1 - T_i) Y_i^S(0) \right)^\top \right) \\ &+ \left(\frac{n_t}{n} - \frac{n_t^2}{n^2} \right) \left(\frac{1}{n_t} \sum T_i Y_i^S(1) \right) \left(\frac{1}{n_t} \sum T_i Y_i^S(1) \right)^\top \\ &- \frac{n_t n_c}{n^2} \left(\frac{1}{n_t} \sum T_i Y_i^S(1) \right) \left(\frac{1}{n_c} \sum (1 - T_i) Y_i^S(0) \right)^\top \\ &- \frac{n_t n_c}{n^2} \left(\frac{1}{n_c} \sum (1 - T_i) Y_i^S(0) \right) \left(\frac{1}{n_t} \sum T_i Y_i^S(1) \right)^\top \\ &+ \left(\frac{n_c}{n} - \frac{n_c^2}{n^2} \right) \left(\frac{1}{n_c} \sum (1 - T_i) Y_i^S(0) \right) \left(\frac{1}{n_c} \sum (1 - T_i) Y_i^S(0) \right)^\top = \frac{n_t n_c}{n^2} \left(\hat{\Sigma}^S + \hat{\tau}_{\text{DiM}}^S \hat{\tau}_{\text{DiM}}^{S\top} \right) \end{aligned}$$

where $\hat{\tau}_{\text{DiM}}^S$ is defined as in (1) and $\hat{\Sigma}^S$ is defined as in (13). Combining the results, we have

$$\begin{aligned} \frac{1}{n} \sum_i (T_i - (Y_i^S - \bar{Y}^S)^\top \hat{\beta})^2 &= \frac{n_t}{n} - \frac{n_t n_c}{n^2} \cdot \hat{\tau}_{\text{DiM}}^{S\top} \left(\hat{\Sigma}^S + \hat{\tau}_{\text{DiM}}^S \hat{\tau}_{\text{DiM}}^{S\top} \right)^{-1} \hat{\tau}_{\text{DiM}}^S \\ &= \frac{n_t}{n} - \frac{n_t n_c}{n^2} \cdot \frac{\hat{\tau}_{\text{DiM}}^{S\top} (\hat{\Sigma}^S)^{-1} \hat{\tau}_{\text{DiM}}^S}{1 + \hat{\tau}_{\text{DiM}}^{S\top} (\hat{\Sigma}^S)^{-1} \hat{\tau}_{\text{DiM}}^S}, \end{aligned}$$

where we apply Sherman-Morrison formula for the second equality.

Now let us show the equation (14). Note that

$$\begin{aligned} & \sum_i W_i (T_i - (Y_i^S - \bar{Y}^S)^\top \hat{\beta})^2 \\ &= \sum W_i T_i - \sum W_i T_i (Y_i^S - \bar{Y}^S)^\top \left(\sum W_i (Y_i^S - \bar{Y}^S)(Y_i^S - \bar{Y}^S)^\top \right)^{-1} \sum W_i T_i (Y_i^S - \bar{Y}^S). \end{aligned}$$

We have that

$$\frac{1}{n} \sum W_i T_i (Y_i^S - \bar{Y}^S) = \frac{n_c}{n_t} \left(\frac{1}{n_t} \sum T_i Y_i^S(1) - \frac{1}{n_c} \sum (1 - T_i) Y_i^S(0) \right).$$

Moreover, we get that

$$\begin{aligned} & \frac{1}{n} \sum W_i (Y_i^S - \bar{Y}^S) (Y_i^S - \bar{Y}^S)^\top \\ &= \frac{1}{n} \sum W_i Y_i^S Y_i^{S\top} - \left(\frac{1}{n} \sum W_i Y_i^S \right) \bar{Y}^{S\top} - \bar{Y}^S \left(\frac{1}{n} \sum W_i Y_i^S \right)^\top + \left(\frac{1}{n} \sum W_i \right) \bar{Y}^S \bar{Y}^{S\top} \\ &= \frac{n}{n_t} \left(\frac{1}{n_t} \sum T_i Y_i^S(1) Y_i^{S\top}(1) - \left(\frac{1}{n_t} \sum T_i Y_i^S(1) \right) \left(\frac{1}{n_t} \sum T_i Y_i^S(1) \right)^\top \right) \\ &+ \frac{n}{n_c} \left(\frac{1}{n_c} \sum (1 - T_i) Y_i^S(0) Y_i^{S\top}(0) - \left(\frac{1}{n_c} \sum (1 - T_i) Y_i^S(0) \right) \left(\frac{1}{n_c} \sum (1 - T_i) Y_i^S(0) \right)^\top \right) \\ &+ \left(\frac{n}{n_t} - 2W(1) \frac{n_t^2}{n^2} + \left(\frac{n}{n_t} + \frac{n}{n_c} \right) \frac{n_t^2}{n^2} \right) \left(\frac{1}{n_t} \sum T_i Y_i^S(1) \right) \left(\frac{1}{n_t} \sum T_i Y_i^S(1) \right)^\top \\ &- \left(W(1) \frac{n_t n_c}{n^2} + W(0) \frac{n_t n_c}{n^2} - \left(\frac{n}{n_t} + \frac{n}{n_c} \right) \frac{n_t n_c}{n^2} \right) \left(\frac{1}{n_t} \sum T_i Y_i^S(1) \right) \left(\frac{1}{n_c} \sum (1 - T_i) Y_i^S(0) \right)^\top \\ &- \left(W(0) \frac{n_t n_c}{n^2} + W(1) \frac{n_t n_c}{n^2} - \left(\frac{n}{n_t} + \frac{n}{n_c} \right) \frac{n_t n_c}{n^2} \right) \left(\frac{1}{n_c} \sum (1 - T_i) Y_i^S(0) \right) \left(\frac{1}{n_t} \sum T_i Y_i^S(1) \right)^\top \\ &+ \left(\frac{n}{n_c} - 2W(0) \frac{n_c^2}{n^2} + \left(\frac{n}{n_t} + \frac{n}{n_c} \right) \frac{n_c^2}{n^2} \right) \left(\frac{1}{n_c} \sum (1 - T_i) Y_i^S(0) \right) \left(\frac{1}{n_c} \sum (1 - T_i) Y_i^S(0) \right)^\top \\ &= \hat{\Sigma}_{\text{DiM}}^S + \left(\frac{n_c}{n_t} + \frac{n_t}{n_c} - 1 \right) \hat{\tau}_{\text{DiM}}^S \hat{\tau}_{\text{DiM}}^{S\top} \end{aligned}$$

where $\hat{\tau}_{\text{DiM}}^S$ is defined as in (1) and $\hat{\Sigma}_{\text{DiM}}^S$ is defined as in (2). Combining the results, we have

$$\begin{aligned} \frac{1}{n} \sum_i W_i (T_i - (Y_i^S - \bar{Y}^S)^\top \hat{\beta})^2 &= \frac{n}{n_t} - \frac{n_c^2}{n_t^2} \cdot \hat{\tau}_{\text{DiM}}^{S\top} \left(\hat{\Sigma}_{\text{DiM}}^S + \left(\frac{n_c}{n_t} + \frac{n_t}{n_c} - 1 \right) \hat{\tau}_{\text{DiM}}^S \hat{\tau}_{\text{DiM}}^{S\top} \right)^{-1} \hat{\tau}_{\text{DiM}}^S \\ &= \frac{n}{n_t} - \frac{n_c^2}{n_t^2} \cdot \frac{\hat{\tau}_{\text{DiM}}^{S\top} (\hat{\Sigma}_{\text{DiM}}^S)^{-1} \hat{\tau}_{\text{DiM}}^S}{1 + \left(\frac{n_c}{n_t} + \frac{n_t}{n_c} - 1 \right) \cdot \hat{\tau}_{\text{DiM}}^{S\top} (\hat{\Sigma}_{\text{DiM}}^S)^{-1} \hat{\tau}_{\text{DiM}}^S}, \end{aligned}$$

where we apply Sherman-Morrison formula for the second equality.

B Proofs for Section 5.2

B.1 RE conditions for sample covariance matrices

Let the sample covariance matrix of Z for the treated group be

$$\hat{\Sigma}_Z^1 = \frac{1}{n_t} \sum_{i:T_i=1} \left(Z_i - \frac{1}{n_t} \sum_{i:T_i=1} Z_i(1) \right) \left(Z_i - \frac{1}{n_t} \sum_{i:T_i=1} Z_i(1) \right)^\top.$$

The sample covariance matrix of Z for the controlled group, $\hat{\Sigma}_Z^0$ is defined similarly.

Set $0 < \theta < 1$. Assume $r \cdot n \geq C \cdot s^* \log p$ for some sufficiently large $C > 0$. Suppose Assumption 2 and Assumption 5 hold. Using Theorem 1.6 in Zhou (2009), we have that $\hat{\Sigma}_Z^1$ satisfies the RE $(s^*, 3, \hat{\Sigma}_Z^1)$ condition with parameter $\kappa_1 := \kappa(s^*, 3, \hat{\Sigma}_Z^1) = (1 - \theta) \cdot \kappa(s^*, 3, \Sigma_Z^1)$ and $\hat{\Sigma}_Z^0$ satisfies the RE $(s^*, 3, \hat{\Sigma}_Z^0)$ condition with parameter $\kappa_0 := \kappa(s^*, 3, \hat{\Sigma}_Z^0) = (1 - \theta) \cdot \kappa(s^*, 3, \Sigma_Z^0)$, with probability at least $1 - 2 \exp(-c\theta^2 n)$ for some constant $c > 0$.

B.2 Concentration inequalities for proofs

In this section, we study concentration inequalities that will be useful for proving Theorem 1. First, consider the matrix,

$$\frac{1}{n} \sum_{i=1}^n W_i (Z_i - \bar{Z})(Z_i - \bar{Z})^\top = \frac{n}{n_t} \hat{\Sigma}_Z^1 + \frac{n}{n_c} \hat{\Sigma}_Z^0 + \left(\frac{n_c}{n_t} + \frac{n_t}{n_c} - 1 \right) \hat{\tau}_Z \hat{\tau}_Z^\top,$$

where the equality comes from calculations in Section A. Note that

$$\begin{aligned} & \left\| \frac{1}{n} \sum_{i=1}^n W_i (Z_i - \bar{Z})(Z_i - \bar{Z})^\top - \frac{1}{\pi} \Sigma_Z^1 - \frac{1}{1-\pi} \Sigma_Z^0 - \left(\frac{1-\pi}{\pi} + \frac{\pi}{1-\pi} - 1 \right) \tau_Z \tau_Z^\top \right\|_\infty \\ & \leq \left\| \frac{n}{n_t} \hat{\Sigma}_Z^1 - \frac{1}{\pi} \Sigma_Z^1 \right\|_\infty + \left\| \frac{n}{n_c} \hat{\Sigma}_Z^0 - \frac{1}{1-\pi} \Sigma_Z^0 \right\|_\infty \\ & \quad + \left\| \left(\frac{n_c}{n_t} + \frac{n_t}{n_c} - 1 \right) \hat{\tau}_Z \hat{\tau}_Z^\top - \left(\frac{1-\pi}{\pi} + \frac{\pi}{1-\pi} - 1 \right) \tau_Z \tau_Z^\top \right\|_\infty, \end{aligned} \quad (15)$$

where $\tau_Z = E[Z(1) - Z(0)]$. In the following, we obtain the concentration inequality for (15).

By Hoeffding's inequality, we have

$$\mathbb{P} \left(\left| \frac{n_t}{n} - \pi \right| > t_n \right) \leq 2 \exp(-2nt_n^2).$$

Then with probability at least $1 - 2 \exp(-2nt_n^2)$, we have

$$\left| \frac{n}{n_t} - \frac{1}{\pi} \right| = \left| \frac{n}{n_t} \left(\frac{n_t}{n} - \pi \right) \frac{1}{\pi} \right| \leq \frac{1}{\pi - \left| \frac{n_t}{n} - \pi \right|} \cdot \frac{1}{\pi} \cdot \left| \frac{n_t}{n} - \pi \right| \leq \frac{t_n}{\pi^2/2}$$

for sufficiently large n with $t_n \rightarrow 0$. Similarly, we can show that

$$\left| \frac{n}{n_t} - \frac{1}{\pi} \right|, \left| \frac{n}{n_c} - \frac{1}{1-\pi} \right|, \left| \frac{n_c}{n_t} - \frac{1-\pi}{\pi} \right|, \left| \frac{n_t}{n_c} - \frac{\pi}{1-\pi} \right| \leq C \cdot t_n \quad (16)$$

for some constant $C > 0$ with probability at least $1 - 2 \exp(-2nt_n^2)$.

Back to (15), by triangular inequality, we get

$$\left\| \frac{n}{n_t} \hat{\Sigma}_Z^1 - \frac{1}{\pi} \Sigma_Z^1 \right\|_\infty \leq \left| \frac{n}{n_t} - \frac{1}{\pi} \right| \cdot \|\Sigma_Z^1\|_\infty + \frac{1}{\pi} \|\hat{\Sigma}_Z^1 - \Sigma_Z^1\|_\infty + \left| \frac{n}{n_t} - \frac{1}{\pi} \right| \cdot \|\hat{\Sigma}_Z^1 - \Sigma_Z^1\|_\infty.$$

Similarly, we can bound the other terms in (15). This tells us that we now need tail bounds for

$$\|\hat{\tau}_Z - \tau\|_\infty, \|\hat{\Sigma}_Z^0 - \Sigma_Z^0\|_\infty, \|\hat{\Sigma}_Z^1 - \Sigma_Z^1\|_\infty, \|\hat{\tau}_Z \hat{\tau}_Z^\top - \tau \tau^\top\|_\infty.$$

Using the Assumption 2, for each $j = 1, \dots, d$, we have the following tail bound,

$$\begin{aligned} \mathbb{P}(|\hat{\tau}_{Zj} - \tau_j| \geq t_n) & \leq \mathbb{P} \left(|\overline{Z_j(1)} - \mathbb{E}[Z_j(1)]| + |\overline{Z_j(0)} - \mathbb{E}[Z_j(0)]| \geq t_n \right) \\ & \leq \mathbb{P} \left(|\overline{Z_j(1)} - \mathbb{E}[Z_j(1)]| \geq t_n/2 \right) + \mathbb{P} \left(|\overline{Z_j(0)} - \mathbb{E}[Z_j(0)]| \geq t_n/2 \right) \\ & \leq 2 \exp \left(-\frac{n_t t_n^2}{8(\sigma_Z^1)^2 (\Sigma_Z^1)_{jj}} \right) + 2 \exp \left(-\frac{n_c t_n^2}{8(\sigma_Z^0)^2 (\Sigma_Z^0)_{jj}} \right) \\ & \leq 4 \exp \left(-\frac{r n t_n^2}{8((\sigma_Z^1)^2 \max_j (\Sigma_Z^1)_{jj} + (\sigma_Z^0)^2 \max_j (\Sigma_Z^0)_{jj})} \right). \end{aligned}$$

By union bound, we have that

$$\mathbb{P}(\|\hat{\tau}_Z - \tau\|_\infty \geq t_n) \leq 4 \exp \left(-\frac{r n t_n^2}{8((\sigma_Z^1)^2 \max_j (\Sigma_Z^1)_{jj} + (\sigma_Z^0)^2 \max_j (\Sigma_Z^0)_{jj})} + \log p \right). \quad (17)$$

Using the Assumption 2 and Lemma 1 in Ravikumar et al. (2011), we again have the tail bound

$$\mathbb{P}\left(|(\hat{\Sigma}_Z^1)_{ij} - (\Sigma_Z^1)_{ij}| \geq t_n\right) \leq 4 \exp\left(-\frac{rnt_n^2}{128(1 + 4(\sigma_Z^1)^2)^2 \max_j((\Sigma_Z^1)_{jj})^2}\right).$$

By union bound, we have that

$$\mathbb{P}\left(\|\hat{\Sigma}_Z^1 - \Sigma_Z^1\|_\infty \geq t_n\right) \leq 4 \exp\left(-\frac{rnt_n^2}{128(1 + 4(\sigma_Z^1)^2)^2 \max_j((\Sigma_Z^1)_{jj})^2} + 2 \log p\right). \quad (18)$$

Similarly, we have that

$$\mathbb{P}\left(\|\hat{\Sigma}_Z^0 - \Sigma_Z^0\|_\infty \geq t_n\right) \leq 4 \exp\left(-\frac{rnt_n^2}{128(1 + 4(\sigma_Z^0)^2)^2 \max_j((\Sigma_Z^0)_{jj})^2} + 2 \log p\right). \quad (19)$$

Moreover, we get

$$\begin{aligned} \mathbb{P}(|\hat{\tau}_{Zi}\hat{\tau}_{Zj} - \tau_i\tau_j| \geq t_n) &\leq \mathbb{P}(|\hat{\tau}_{Zi} - \tau_i| \cdot |\hat{\tau}_{Zj} - \tau_j| + |\tau_i| \cdot |\hat{\tau}_{Zj} - \tau_j| + |\tau_j| \cdot |\hat{\tau}_{Zi} - \tau_i| \geq t_n) \\ &\leq \mathbb{P}(|\hat{\tau}_{Zi} - \tau_i| \cdot |\hat{\tau}_{Zj} - \tau_j| \geq t_n/3) \\ &\quad + \mathbb{P}(|\tau_i| \cdot |\hat{\tau}_{Zj} - \tau_j| \geq t_n/3) + \mathbb{P}(|\tau_j| \cdot |\hat{\tau}_{Zi} - \tau_i| \geq t_n/3) \\ &\leq 8 \exp\left(-\frac{rnt_n}{6((\sigma_Z^1)^2 \max_j(\Sigma_Z^1)_{jj} + (\sigma_Z^0)^2 \max_j(\Sigma_Z^0)_{jj})}\right) \\ &\quad + 8 \exp\left(-\frac{rnt_n^2}{18 \max_j |\tau_j|^2 ((\sigma_Z^1)^2 \max_j(\Sigma_Z^1)_{jj} + (\sigma_Z^0)^2 \max_j(\Sigma_Z^0)_{jj})}\right) I\left(\max_j |\tau_j| > 0\right). \end{aligned}$$

Similarly, we apply the union bound to get the following tail bound

$$\begin{aligned} \mathbb{P}(\|\hat{\tau}_Z \hat{\tau}_Z^\top - \tau \tau^\top\|_\infty \geq t_n) &\leq 8 \exp\left(-\frac{rnt_n}{6((\sigma_Z^1)^2 \max_j(\Sigma_Z^1)_{jj} + (\sigma_Z^0)^2 \max_j(\Sigma_Z^0)_{jj})} + 2 \log p\right) \\ &\quad + 8 \exp\left(-\frac{rnt_n^2}{18 \max_j |\tau_j|^2 ((\sigma_Z^1)^2 \max_j(\Sigma_Z^1)_{jj} + (\sigma_Z^0)^2 \max_j(\Sigma_Z^0)_{jj})} + 2 \log p\right) I\left(\max_j |\tau_j| > 0\right). \end{aligned} \quad (20)$$

Let $t_n \geq A\sqrt{\log p/n}$ where $A > 1$ is sufficiently large enough to ensure that exponential factors in (17), (18), (19), and (20) are negative. Combining results in (16), (17), (18), (19), and (20), we have

$$(15) \leq C \cdot t_n$$

with probability at least $1 - c_1 \exp(-c_2 nt_n^2)$ for some constants $C, c_1, c_2 > 0$.

Similarly, we can get

$$\begin{aligned} &\left\|\frac{1}{n} \sum_{i=1}^n W_i(Z_i - \bar{Z})(X_i - \bar{X})^\top - \frac{1}{\pi} \text{Cov}(Z(1), X) - \frac{1}{1-\pi} \text{Cov}(Z(0), X)\right\|_\infty \\ &= \left\|\frac{1}{n} \sum_{i=1}^n W_i(Z_i - \bar{Z})(X_i - \bar{X})^\top\right\|_\infty \leq C \cdot t_n \end{aligned} \quad (21)$$

$$\left\|\frac{1}{n} \sum_{i=1}^n W_i(X_i - \bar{X})(X_i - \bar{X})^\top - \frac{1}{\pi(1-\pi)} \Sigma_X\right\|_\infty \leq C \cdot t_n \quad (22)$$

with probability at least $1 - c_1 \exp(-c_2 nt_n^2)$ for some constants $C, c_1, c_2 > 0$.

Moreover, since the pre-treatment covariates dimension m is fixed, using the matrix Bernstein inequality (Wainwright, 2019), we get

$$\left\|\frac{1}{n} \sum_{i=1}^n W_i(X_i - \bar{X})(X_i - \bar{X})^\top - \frac{1}{\pi(1-\pi)} \Sigma_X\right\|_2 \leq C \cdot t_n \quad (23)$$

$$\left\| \frac{1}{n} \sum_{i=1}^n W_i T_i (X_i - \bar{X}) \right\|_2 \leq C \cdot t_n \quad (24)$$

$$\left\| \frac{1}{n} \sum_{i=1}^n W_i (X_i - \bar{X}) (Y_{ij} - \bar{Y}_j)^\top - \frac{1}{\pi} \text{Cov}(X, Y_j(1)) - \frac{1}{1-\pi} \text{Cov}(X, Y_j(0)) \right\|_2 \leq C \cdot t_n \quad (25)$$

for $j = 1, \dots, p$, with probability at least $1 - c_1 \exp(-c_2 n t_n^2)$ for some constants $C, c_1, c_2 > 0$.

B.3 Proof of Theorem 1

Note that

$$\hat{\alpha} = \left[\frac{1}{n} \sum_{i=1}^n W_i (X_i - \bar{X}) (X_i - \bar{X})^\top \right]^{-1} \left(\frac{1}{n} \sum_{i=1}^n W_i (X_i - \bar{X}) T_i - \frac{1}{n} \sum_{i=1}^n W_i (X_i - \bar{X}) (Y_i - \bar{Y})^\top \beta \right).$$

Let

$$\begin{aligned} \hat{b} &= \left[\frac{1}{n} \sum_{i=1}^n W_i (X_i - \bar{X}) (X_i - \bar{X})^\top \right]^{-1} \frac{1}{n} \sum_{i=1}^n W_i (X_i - \bar{X}) T_i \\ \hat{A} &= \left[\frac{1}{n} \sum_{i=1}^n W_i (X_i - \bar{X}) (X_i - \bar{X})^\top \right]^{-1} \frac{1}{n} \sum_{i=1}^n W_i (X_i - \bar{X}) (Y_i - \bar{Y})^\top. \end{aligned}$$

The following lemma gives the concentration inequalities for \hat{b} and \hat{A} . The proof of the Lemma 1 can be found in Section B.5.

Lemma 1. *There exist positive constants b_1, b_2, a_1, a_2 such that*

$$\begin{aligned} \mathbb{P} \left(\|\hat{b}\|_1 \geq t_n \right) &\leq b_1 \exp(-b_2 n t_n^2) \\ \mathbb{P} \left(\max_{j=1}^p \|\hat{A}_j - A_j\|_1 \geq t_n \right) &\leq a_1 \exp(-a_2 n t_n^2 + \log p). \end{aligned}$$

where \hat{A}_j is the j -th column of \hat{A} and A_j is defined as

$$A_j := (1 - \pi) \text{Var}(X)^{-1} \text{Cov}(X, Y_j(1)) + \pi \text{Var}(X)^{-1} \text{Cov}(X, Y_j(0)).$$

Note that $\hat{\beta}$ can be written as

$$\begin{aligned} \hat{\beta} &= \arg \min_{\beta} \frac{1}{n} \sum_i W_i (T_i - (X_i - \bar{X})^\top \hat{b} - [(Y_i - \bar{Y}) - \hat{A}^\top (X_i - \bar{X})]^\top \beta)^2 + 2\lambda_n \|\beta\|_1 \\ &= \arg \min_{\beta} \frac{1}{n} \sum_i W_i (T_i - (X_i - \bar{X})^\top \hat{b} - [(Z_i - \bar{Z}) - (\hat{A} - A)^\top (X_i - \bar{X})]^\top \beta)^2 + 2\lambda_n \|\beta\|_1. \end{aligned} \quad (26)$$

From the sub-differential property of the minimizer in (26), we have

$$\begin{aligned} \left\| \frac{1}{n} \sum_{i=1}^n W_i \left(Z_i - \bar{Z} - (\hat{A} - A)^\top (X_i - \bar{X}) \right) \right. \\ \left. \left(T_i - (X_i - \bar{X})^\top \hat{b} - [Z_i - \bar{Z} - (\hat{A} - A)^\top (X_i - \bar{X})]^\top \hat{\beta} \right) \right\|_\infty \leq \lambda_n. \end{aligned} \quad (27)$$

Set $\delta = \hat{\beta} - \beta^*$ and $J_0 = J(\beta^*)$. By Lemma 1 in Negahban et al. (2009), if

$$\begin{aligned} \left\| \frac{1}{n} \sum_{i=1}^n W_i \left(Z_i - \bar{Z} - (\hat{A} - A)^\top (X_i - \bar{X}) \right) \right. \\ \left. \left(T_i - (X_i - \bar{X})^\top \hat{b} - [Z_i - \bar{Z} - (\hat{A} - A)^\top (X_i - \bar{X})]^\top \beta^* \right) \right\|_\infty \leq \lambda_n, \end{aligned} \quad (28)$$

then δ satisfies

$$\|\delta_{J_0^c}\|_1 \leq 3\|\delta_{J_0}\|_1.$$

We first state the lemma saying that (28) holds with high probability. The proof can be found in Section B.4.

Lemma 2. *Suppose the assumptions of Theorem 1 hold. Let $\lambda_n \geq A\sqrt{\log p/n}$ for some sufficiently large $A > 0$. Then with probability at least $1 - c_1 \exp(-c_2 n \lambda_n^2)$ for some positive constants c_1, c_2 , we have the inequality (28).*

With the choice of λ_n in Lemma 2, from (27) and (28), we have that

$$\left\| \frac{1}{n} \sum_{i=1}^n W_i \left(Z_i - \bar{Z} - (\hat{A} - A)^\top (X_i - \bar{X}) \right) \left(Z_i - \bar{Z} - (\hat{A} - A)^\top (X_i - \bar{X}) \right)^\top \delta \right\|_\infty \leq 2\lambda_n,$$

with probability at least $1 - c_1 \exp(-c_2 n \lambda_n^2)$ for some positive constants $c_1, c_2 > 0$. Then, we get that

$$\begin{aligned} \left\| \frac{1}{n} \sum_{i=1}^n W_i (Z_i - \bar{Z}) (Z_i - \bar{Z})^\top \delta \right\|_\infty &\leq 2\lambda_n + 2 \left\| \frac{1}{n} \sum_{i=1}^n W_i (Z_i - \bar{Z}) (X_i - \bar{X})^\top (\hat{A} - A) \right\|_\infty \|\delta\|_1 \\ &\quad + \left\| (\hat{A} - A)^\top \frac{1}{n} \sum_{i=1}^n W_i (X_i - \bar{X}) (X_i - \bar{X})^\top (\hat{A} - A) \right\|_\infty \|\delta\|_1 \\ &\leq 2\lambda_n + 3\lambda_n^2 \|\delta\|_1, \end{aligned}$$

where the last inequality comes from (21), (22), and Lemma 1. Therefore,

$$\begin{aligned} \delta^\top \left(\frac{1}{n} \sum_i W_i (Z_i - \bar{Z}) (Z_i - \bar{Z})^\top \right) \delta &\leq \left\| \frac{1}{n} \sum_{i=1}^n W_i (Z_i - \bar{Z}) (Z_i - \bar{Z})^\top \delta \right\|_\infty \|\delta\|_1 \\ &\leq 2\lambda_n \|\delta\|_1 + 3\lambda_n^2 \|\delta\|_1^2 \\ &\leq 8\sqrt{s^*} \lambda_n \|\delta_{J_0}\|_2 + 48s^* \lambda_n^2 \|\delta_{J_0}\|_2^2. \end{aligned}$$

From the RE assumption in Section B.1, we have

$$\begin{aligned} \delta^\top \left(\frac{1}{n} \sum_i W_i (Z_i - \bar{Z}) (Z_i - \bar{Z})^\top \right) \delta &\geq \delta^\top \left(\frac{n}{n_t} \hat{\Sigma}_Z^1 + \frac{n}{n_c} \hat{\Sigma}_Z^0 \right) \delta \\ &\geq (\kappa_1 + \kappa_0) \|\delta_{J_0}\|_2^2 / (1 - r). \end{aligned}$$

Combining these results, we have

$$(\kappa_1 + \kappa_0) \|\delta_{J_0}\|_2 \leq 8\sqrt{s^*} \lambda_n + 48s^* \lambda_n^2 \|\delta_{J_0}\|_2.$$

Given that $n \gg s^* \log p$, we have

$$\frac{(\kappa_1 + \kappa_0)}{2} \|\delta_{J_0}\|_2 \leq 8\sqrt{s^*} \lambda_n.$$

Then, we have

$$\|\delta\|_1 = \|\delta_{J_0}\|_1 + \|\delta_{J_0^c}\|_1 \leq 4\|\delta_{J_0}\|_1 \leq 4\sqrt{s^*} \|\delta_{J_0}\|_2 \leq \frac{64\lambda_n s^*}{\kappa_1 + \kappa_0}.$$

Then the recovery result follows from the fact that the bound on the ℓ_1 -distance gives the identical bound on the ℓ_∞ -distance between $\hat{\beta}$ and β^* . This completes the proof.

B.4 Proofs of Lemma 2

In this Section, we prove Lemma 2. Note that

the left hand side of (28)

$$\begin{aligned}
&\leq \left\| \frac{1}{n} \sum_{i=1}^n W_i(Z_i - \bar{Z})(T_i - (Z_i - \bar{Z})^\top \beta^*) \right\|_\infty \\
&+ \left\| \frac{1}{n} \sum_{i=1}^n W_i(Z_i - \bar{Z})(X_i - \bar{X})^\top \hat{b} \right\|_\infty + \left\| (\hat{A} - A)^\top \frac{1}{n} \sum_{i=1}^n W_i(X_i - \bar{X}) T_i \right\|_\infty \\
&+ \left\| (\hat{A} - A)^\top \frac{1}{n} \sum_{i=1}^n W_i(X_i - \bar{X})(X_i - \bar{X})^\top \hat{b} \right\|_\infty \\
&+ 2 \cdot \left\| \frac{1}{n} \sum_{i=1}^n W_i(Z_i - \bar{Z})(X_i - \bar{X})^\top (\hat{A} - A) \right\|_\infty \|\beta^*\|_1 \\
&+ \left\| (\hat{A} - A)^\top \frac{1}{n} \sum_{i=1}^n W_i(X_i - \bar{X})(X_i - \bar{X})^\top (\hat{A} - A) \right\|_\infty \|\beta^*\|_1 \\
&\leq \left\| \frac{1}{n} \sum_{i=1}^n W_i(Z_i - \bar{Z})(T_i - (Z_i - \bar{Z})^\top \beta^*) \right\|_\infty \tag{29}
\end{aligned}$$

$$+ \|\hat{b}\|_1 \cdot \left\| \frac{1}{n} \sum_{i=1}^n W_i(Z_i - \bar{Z})(X_i - \bar{X})^\top \right\|_\infty \tag{30}$$

$$+ \left(\max_{j=1}^d \|\hat{A}_j - A_j\|_1 \right) \cdot \left(\left\| \frac{1}{n} \sum_{i=1}^n W_i(X_i - \bar{X}) T_i \right\|_\infty + 2 \left\| \frac{1}{n} \sum_{i=1}^n W_i(Z_i - \bar{Z})(X_i - \bar{X})^\top \right\|_\infty \|\beta^*\|_1 \right) \tag{31}$$

$$+ \|\hat{b}\|_1 \cdot \left(\max_{j=1}^d \|\hat{A}_j - A_j\|_1 \right) \cdot \left\| \frac{1}{n} \sum_{i=1}^n W_i(X_i - \bar{X})(X_i - \bar{X})^\top \right\|_\infty \tag{32}$$

$$+ \left(\max_{j=1}^d \|\hat{A}_j - A_j\|_1 \right)^2 \cdot \left\| \frac{1}{n} \sum_{i=1}^n W_i(X_i - \bar{X})(X_i - \bar{X})^\top \right\|_\infty \|\beta^*\|_1. \tag{33}$$

Let's start with (29). Note that from the calculations in Section A, we get

$$\begin{aligned}
&\left\| \frac{1}{n} \sum_{i=1}^n W_i(Z_i - \bar{Z})(T_i - (Z_i - \bar{Z})^\top \beta^*) \right\|_\infty \\
&= \left\| \frac{n_c}{n_t} \hat{\tau}_Z - \left(\frac{n}{n_t} \hat{\Sigma}_Z^1 + \frac{n}{n_c} \hat{\Sigma}_Z^0 + \left(\frac{n_c}{n_t} + \frac{n_t}{n_c} - 1 \right) \hat{\tau}_Z \hat{\tau}_Z^\top \right) \beta^* \right\|_\infty \\
&\leq \left\| \frac{n_c}{n_t} \hat{\tau}_Z - \frac{1-\pi}{\pi} \tau \right\|_\infty + \left\| \frac{n}{n_t} \hat{\Sigma}_Z^1 - \frac{1}{\pi} \Sigma_Z^1 \right\|_\infty \|\beta^*\|_1 + \left\| \frac{n}{n_c} \hat{\Sigma}_Z^0 - \frac{1}{1-\pi} \Sigma_Z^0 \right\|_\infty \|\beta^*\|_1 \\
&\quad + \left\| \left(\frac{n_c}{n_t} + \frac{n_t}{n_c} - 1 \right) \cdot \hat{\tau}_Z \hat{\tau}_Z^\top - \left(\frac{1-\pi}{\pi} + \frac{\pi}{1-\pi} - 1 \right) \tau \tau^\top \right\|_\infty \|\beta^*\|_1.
\end{aligned}$$

From Section B.2, with $t_n \geq A\sqrt{\log p/n}$ for sufficiently large $A > 1$,

$$(29) \leq M \cdot t_n$$

with probability at least $1 - c_1 \exp(-c_2 n t_n^2)$ for some constants $M, c_1, c_2 > 0$.

Similarly, using results from Section B.2 and Lemma 1, we have that

$$(30), (31), (32), (33) \leq 2t_n^2(1 + \|\beta^*\|_1)(M + t_n)$$

with probability at least $1 - c_1 \exp(-c_2 n t_n^2)$ for some constants $M, c_1, c_2 > 0$.

Eventually, combining all the results, we have

$$\text{the left hand side of (28)} \leq \lambda_n$$

for $\lambda_n \geq A\sqrt{\log p/n}$ for some sufficiently large $A > 1$, with probability at least $1 - c_1 \exp(-c_2 n \lambda_n^2)$ for some constants $c_1, c_2 > 0$. This completes the proof.

B.5 Proof of Lemma 1

Define

$$\begin{aligned}\hat{\Sigma}_X^W &= \pi(1 - \pi) \cdot \frac{1}{n} \sum_{i=1}^n W_i (X_i - \bar{X})(X_i - \bar{X})^\top \\ \hat{\Sigma}_{XY_j}^W &= \pi(1 - \pi) \cdot \frac{1}{n} \sum_{i=1}^n W_i (X_i - \bar{X})(Y_{ij} - \bar{Y}_j)^\top \\ \Sigma_{XY_j} &= (1 - \pi)\text{Cov}(X, Y_j(1)) + \pi\text{Cov}(X, Y_j(0)).\end{aligned}$$

With probability at least $1 - c_1 \exp(-c_2 n t_n^2)$, using (23), we have

$$\begin{aligned}\|\hat{\Sigma}_X^{W^{-1}} - \Sigma_X^{-1}\|_2 &= \|\Sigma_X^{-1}(\hat{\Sigma}_X^W - \Sigma_X)\hat{\Sigma}_X^{W^{-1}}\|_2 \\ &\leq \|\Sigma_X^{-1}\|_2 \|\hat{\Sigma}_X^W - \Sigma_X\|_2 \|\hat{\Sigma}_X^{W^{-1}}\|_2 \\ &\leq \|\Sigma_X\|_2^{-1} \cdot t_n \cdot \frac{1}{\|\Sigma_X\|_2 - t_n} \leq \frac{t_n}{\|\Sigma_X\|_2^2/2}\end{aligned}$$

for sufficiently large n with $t_n \rightarrow 0$. Therefore, using (24), we have

$$\|\hat{b}\|_2 \leq \|\hat{\Sigma}_X^{W^{-1}}\|_2 \left\| \pi(1 - \pi) \cdot \frac{1}{n} \sum_{i=1}^n W_i T_i (X_i - \bar{X}) \right\|_2 \leq \frac{t_n}{\|\Sigma_X\|_2^2/2}$$

and using (25), we get

$$\begin{aligned}\|\hat{A}_j - A_j\|_2 &\leq \|\hat{\Sigma}_X^{W^{-1}} - \Sigma_X^{-1}\|_2 \|\Sigma_{XY_j}\|_2 + \|\Sigma_X^{-1}\|_2 \|\hat{\Sigma}_{XY_j}^W - \Sigma_{XY_j}\|_2 \\ &\quad + \|\hat{\Sigma}_X^{W^{-1}} - \Sigma_X^{-1}\|_2 \|\hat{\Sigma}_{XY_j}^W - \Sigma_{XY_j}\|_2 \\ &\leq C_1 t_n + C_2 t_n^2,\end{aligned}$$

for some constants $C_1, C_2 > 0$. Note that $\|x\|_1 \leq \sqrt{m}\|x\|_2$ for $x \in \mathbb{R}^m$. This completes the proof.

C Additional Simulations

C.1 Without Pre-treatment Covariates

We consider scenarios involving independent outcomes and a constant treatment effect without pre-treatment covariates. We generate the data set as follows.

$$\begin{aligned}Y_{ij} &= \alpha \cdot T_i \cdot I(j \leq s^*) + \epsilon_{ij}, \\ T_i &\stackrel{i.i.d.}{\sim} \text{Bernoulli}(p), \\ \epsilon_{ij} &\stackrel{i.i.d.}{\sim} N(0, 1).\end{aligned}$$

for $i = 1, \dots, n$ and $j = 1, \dots, d$. Note that the outcome dimension is d , and there are non-zero treatment effects on $S^* = \{Y_1, \dots, Y_{s^*}\}$, where the sparsity index is s^* .

The recovery rates of true S^* for the baseline approach and the proposed approach for different sample sizes (n), probabilities of being treated (p), and magnitudes of treatment effects (α) are given in Figure 5. We set the outcome dimension $d = 100$ and the sparsity index $s^* = 5$. Both the baseline approach and the proposed approach show similar performance.

C.2 With Partially-Observable Pre-treatment Covariates

When pre-treatment covariates are partially observable under the simulation model in Section 6.1, the sparsity assumption of the inverse covariance matrix in Section 5.2 is violated. In the following, we add simulation results where we only observe a subset of pre-treatment covariates; we only observe 20 out of $m = 30$. The results are presented in Figure 6. We see that the proposed approach still mostly outperforms the baseline approach, especially when sample sizes are small and signals are weak.

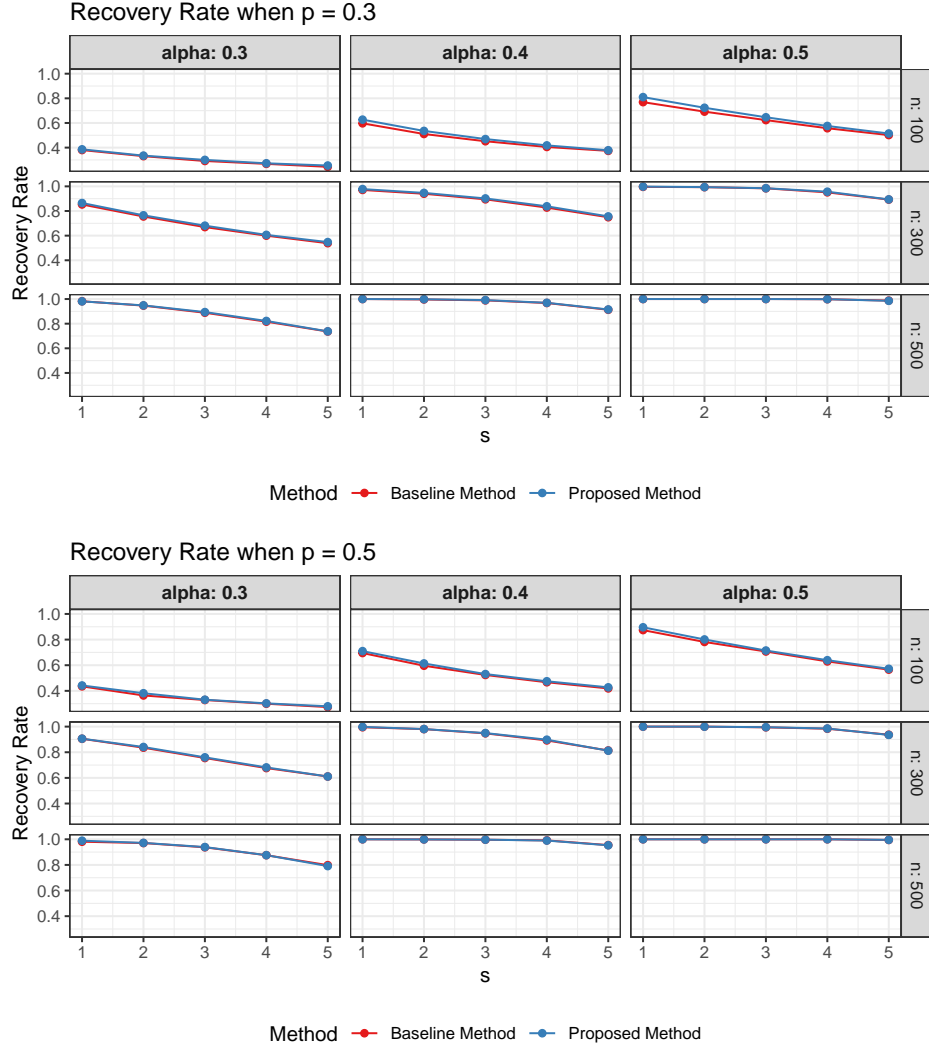


Figure 5: Recovery rates averaged over 1000 replicates for the baseline approach and the proposed approach (without pre-treatment covariates adjustment) for each $n = 100, 300, 500$, $p = 0.3, 0.5$, and $\alpha = 0.3, 0.4, 0.5$ are presented.

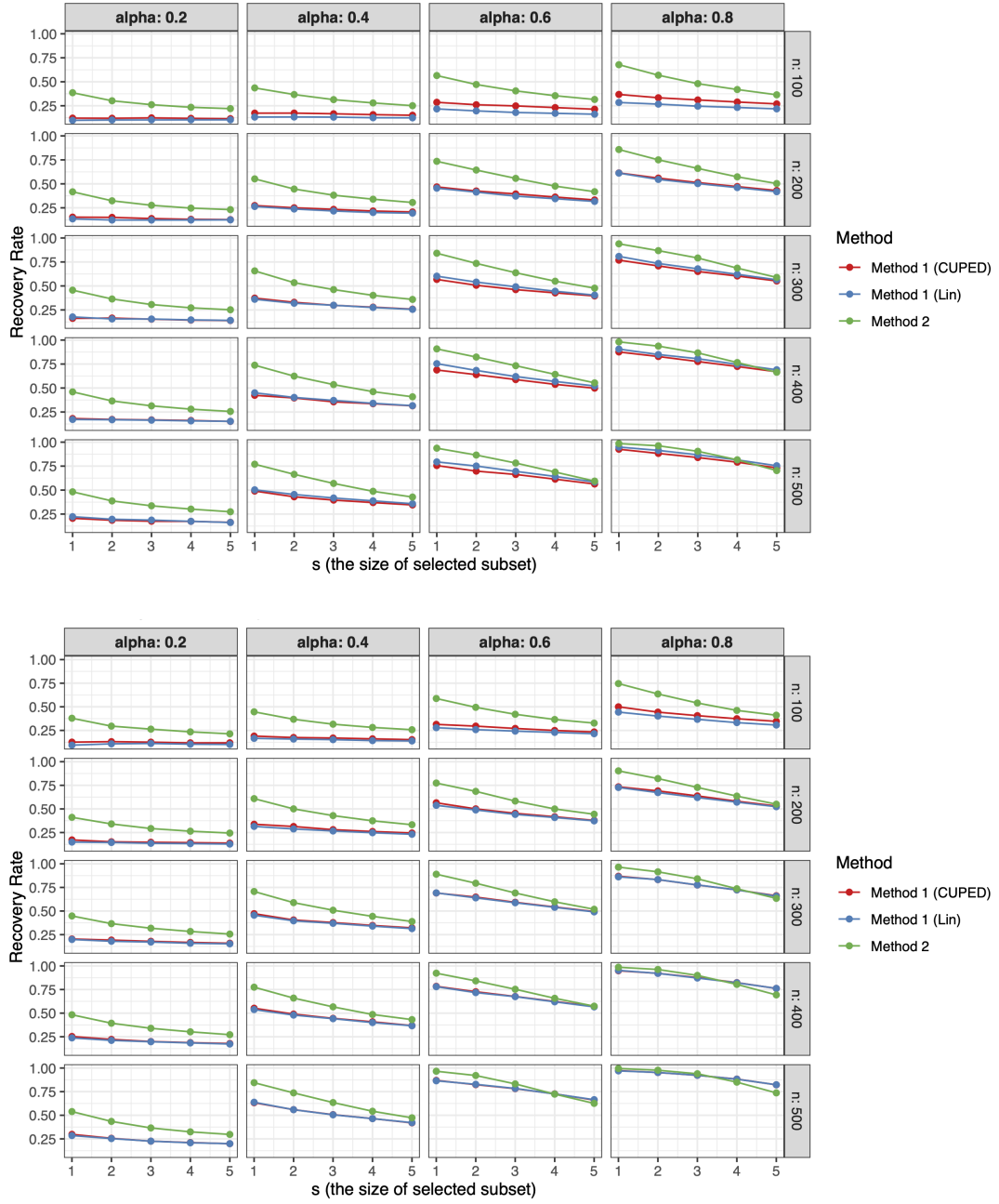


Figure 6: Recovery rates averaged over 1000 replicates for the baseline and proposed approaches with pre-treatment covariates adjustment when pre-treatment covariates are partially observable for $n = 100, 200, 300, 400, 500$ and $\alpha = 0.2, 0.4, 0.6, 0.8$ for $\pi = 0.3$ (Above) and $\pi = 0.5$ (Below).